UNIVERSITA' DEGLI STUDI DI NAPOLI FEDERICO II

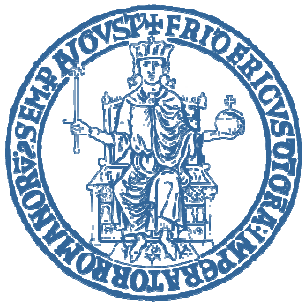

DIPARTIMENTO DI INGEGNERIA ELETTRICA E TECNOLOGIA DELL'INFORMAZIONE

*DOTTORATO DI RICERCA IN INGEGNERIA ELETTRICA*
*XXVII CICLO*

# *EXPERIMENTAL ANALYSIS ON LABORATORY DC FAST CHARGING ARCHITECTURE FOR ELECTRIC AND PLUG-IN HYBRID VEHICLES*

*Tutor:*

Ch.mo Prof. Diego Iannuzzi (DIETI)

Ing. Ottorino Veneri (Istituto Motori - CNR)

*Candidato:*

Ing. Clemente Capasso

MARZO 2015

## Abstract

This manuscript is aimed to present a complete experimental analysis on DC power architecture for fast charging operations of full electric and plug-in hybrid vehicles. The described research activities start from an experimental characterization of energy storage systems of different technologies during their charging and discharging operations. These tests are carried out through a specific laboratory bench, which is properly controlled in order to obtain the required charging/discharging profiles. Then the analysis on the DC charging architecture is performed by means of a laboratory prototype, which has been designed and realized as case study. The analyzed prototype of DC charging station is composed by a 20 kW grid tied AC/DC converter, which realizes the DC-Link starting from the low voltage AC grid, and DC/DC power converters for the connection of vehicles on charge and stationary energy storage buffers. Experimental tests are aimed in this case to characterize and analyze the performance of the considered DC power architecture in different operative conditions. Laboratory results have firstly shown the good behaviour of lithium storage technologies in supporting fast charging/discharging operations. Then the experimental evaluations on the laboratory prototype have shown the effectiveness of the realized control strategies and the real advantages of using DC charging architecture, integrated with energy storage buffers, mainly in terms of efficiency, charging times and impact on the main grid.

## Table of Contents

## Introduction

Nowadays road transportation systems are mainly based on the use of fossil fuels as primary energy sources. In fact, private, public and corporate road vehicles are responsible for about the 60% of global oil consumption. In addition a strong increase in fossil fuels demand, mainly due to the growing number of road vehicles, is expected in the near term future [1] [2]. This scenario of oil dependency involves numerous and relevant issues, which interest environmental, economic and political aspects. In order to address these issues recent advancement in internal combustion engine technologies, also encouraged by new strictly international legislations, have allowed improvements in vehicle conversion efficiencies and tailpipe emissions [3]. Nevertheless worldwide crude oil consumption and the amount of pollutant and greenhouse gases emissions in the earth atmosphere are in continuous grow.

In the above context electric and plug-in hybrid vehicles, which are both commonly referred as plug-in vehicles (PEVs), appear to be a feasible solution to support the transition towards a sustainable mobility, since they are characterized by high well-to-wheel conversion efficiency and no local pollutant emissions As matter of fact the widespread adoption of this kind of vehicles in the road transportation sector is still affected by different enabling factors such as the development of battery technology and the diffusion of a proper charging infrastructure. In this regard recent lithium based energy storage systems have given a strong support to the acceptance of PEVs in private and corporate sectors [4] [5]. This is mainly due to the fact that new lithium compounds are characterized by high values of energy and power densities, which allow supplying PEVs with good performance in terms of acceleration and daily travel range. On the other hand the reduced autonomy is still considered by the great part of the users as the main technical bottleneck of PEVs [6]. As a consequence it is clear that the capillary diffusion of a proper charging infrastructure would be required in order to support the use of PEVs also for long travel distance. In fact in the most of the cases PEVs are charged during the night through private charging equipment, which is generally devoted to the low power operations, characterized by charging times up to 8 hours. This type of recharge can be considered suitable for urban mobility since it allows a daily travel range of about 150 *km* [6]. Longer travel

distances could be obtained with the development of a proper charging infrastructure characterized by the availability of frequent fast charging stations along the road. Unfortunately fast charging operations generally involve high power requirements from the main grid, which might not be able to support simultaneous fast charging operations of different vehicles.

The above issues can be addressed in a smart grid scenario where PEVs can be charged in an efficient and clean way thanks to the intelligent integration of renewable energy sources and stationary energy storage systems supporting the main grid in its interaction with the plug-in mobility. In this regards different architecture are proposed in literature, supported by the related simulation activities and results, with specific focus on the energy management strategies of distributed systems[7][8][9]. On the other hand, the lack of literature knowledge and information on experimental data justifies the interest of the research activities reported in this manuscript towards a laboratory analysis on the real performance of DC fast charging architecture. This analysis is realized by means of a laboratory prototype, which has been properly designed and realized as case study. In addition the above activities are supported by an experimental study on the real behaviour of different vehicle energy storage systems during their charging/discharging operations, in order to evaluate the effect of the charging rate on vehicle expected travel range.

This manuscript starts with a description, reported in Chapter 1, of the smart grid concept and the intelligent integration of renewable energy sources, stationary energy storage systems and PEVs under different aggregative schemes. Then, Chapter 2 analyzes different charging modes and architecture with particular focus on DC power configurations, based on the use of energy storage buffers, which are aimed to mitigate the power requirements of fast charging operations from the main grid. The different PEVs storage technologies are described in detail in Chapter 3, with specific attention on the identification of their main performance parameters. Chapter 3 also introduces the laboratory test bench used for the experimental characterization of different energy storage modules. The laboratory prototype of DC fast charging station is presented in Chapter 4, with a description of the design criteria, converter topologies and control strategies. Chapter 5 reports the experimental results and discussion related to the experimental tests on energy storage modules of different chemistries and to the laboratory analysis on the DC

charging station prototype. Finally conclusions and future works are reported in the last Chapter.

The activities reported in this manuscript have been carried out in collaboration between the Istituto Motori of the National Research Council of Italy and Department of Electrical Engineering and Information Technology of the University of Naples - Federico II.

# **Chapter 1.** Electric and plug-in hybrid vehicles in the smart grid scenario

### *Introduction*

Full Electric and Plug-in Hybrid Electric Vehicles are emerging as one of the most attractive solutions for the growing amount of air pollution related to the public and private road transportation sectors [10].

When PEVs are connected on charge, they are currently considered as a simple load with minimal effects on the daily power demand profile. This is mainly due to the fact that the diffusion of this kind of vehicles is still very low and the existing charging infrastructure is mainly based on low power charging points, which are devoted to slow charging operations generally performed during the night. Nevertheless the electric power system, in its existing configuration, is not ready to face long-term diffusion of PEVs fleets, which are expected to gain more and more market share on the base of different scenarios presented in the literature [11].

For the above reasons a transaction towards a new sustainable distributed architecture involving intelligent management systems is considered as a possible way out in order to avoid large capital investments in network reinforcements. At the same time the smart integration in the existing network of renewable energy sources can give further support to the reduction of pollutant emissions related to traditional energy generation systems.

This Chapter starts with a detailed market penetration analysis related to electric (EVs) and plug-in hybrid (PHEVs) vehicles, with specific focus on the comparison between Italian and International automotive sector. This analysis is aimed to evaluate the main technical bottlenecks and enabling factors for a large scale adoption of these kinds of vehicles. Then the smart grid concept is introduced with a description of its advantages in supporting the integration of PEVs into intelligent and distributed power architecture, characterized by a growing amount of stationary energy storage systems and renewable energy generation units. Finally different smart aggregation, communication and control schemes are presented with the aim of evaluating the possible benefits for the main grid related to the integration and the proper management of a large number of vehicles on charge.

### *1.1 Market penetration analysis of electric and plug-in hybrid vehicles*

In recent years the Italian automotive sector has been affected by a decrease of about 40% in the number of vehicles sold, which have been reduced from 2.2 millions, in the 2005, to 1.3 millions, in the 2013. In this context full electric vehicles (EVs) represent a niche sector with a market share lower than 1%. Nevertheless the number of EVs is growing with a positive trend in comparison with the automotive market behavior. In this regards, Figure 1 reports the number of units sold, from 2005 to 2013, and the market share of this kind of vehicles with reference to Italian automotive sector. In particular, although the percentage of EVs with respect to the whole vehicle market is still very low, a remarkable increase in the number of units sold can be observed from 2009 onwards [12].

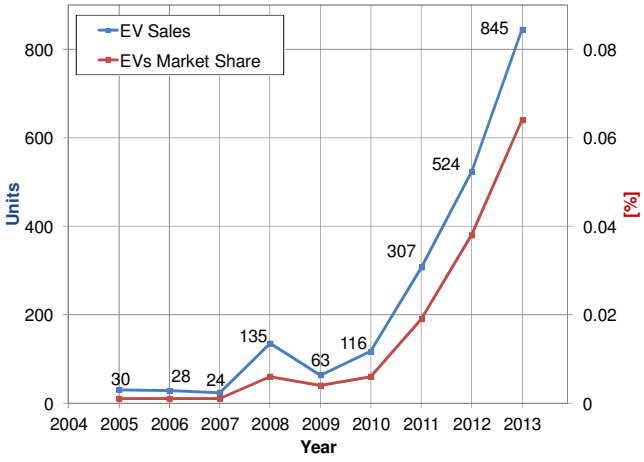


**Figure 1** *Number of units sold and market share for full electric vehicles in Italy.*

From a sector analysis it results that the 80% of EVs market can be assigned to car-rental and/or car-sharing companies. In particular car-sharing is considered a new sector of great interest since it allows users, which are oriented in buying EVs, to carry out preliminary road tests on their performance. As a consequence, car-sharing services can work as a flywheel for the future development of EVs market. Other interesting aspect of these services are mainly related to their advantages in terms of cost, with respect to car-rental or taxi services, and reduction of circulating vehicles on the roads, with positive consequences on the traffic and viability in the urban areas. Moreover, when based on electric mobility, car-sharing and car-rental services allow their users to access limited traffic and parking areas.

Another sector of strong interest is represented by corporate fleets, which are considered responsible for 10%-15% of EVs Italian market share. In fact many companies can take advantage from the acquisition of higher number of vehicles with respect to private users, with consequent facilitation in payment conditions. Other advantages are represented by the return on image for the companies, which adopt corporate fleets based on 'green' mobility. Nevertheless the average travel ranges required are often higher in comparison with the reduced autonomies, characteristic of the electric mobility. This is one of the reasons why the adoption of EVs for corporate fleets is generally limited to applications where the vehicle mission is well known and the required travel distances are low, such as last mile delivery or taxi services,.

The private sector gives the lowest contribution to the EVs market, with an evaluated percentage of about 5% with respect to the sold units of EVs. This is mainly due to their low travel ranges and the lack of a proper public charging infrastructure, which strongly affect private customer's acceptance toward electric mobility.

The increasing market penetration of road EVs in recent years can be justified by the recent availability on the market of a new generation of electric vehicles, which are characterized by innovative design, high travel range up to 200 *km* and attractive costs, when supported by national incentives. In this regard Figure 2 reports the models of electric vehicles sold in Italy in the 2013 [12].

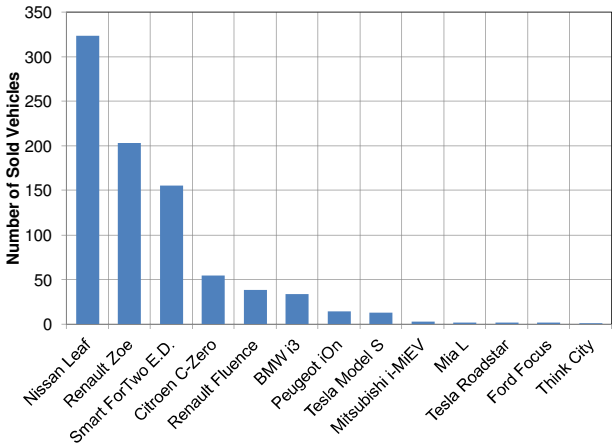


**Figure 2** *Main electric vehicle models sold in Italy in the 2013.*

The market situation for hybrid electric vehicles (HEVs), based on the use of thermal engine and electric dive in different possible configurations, is characterized by higher values of sold vehicles and market share, in comparison to the case of EVs, as reported in Figure 3 [12].

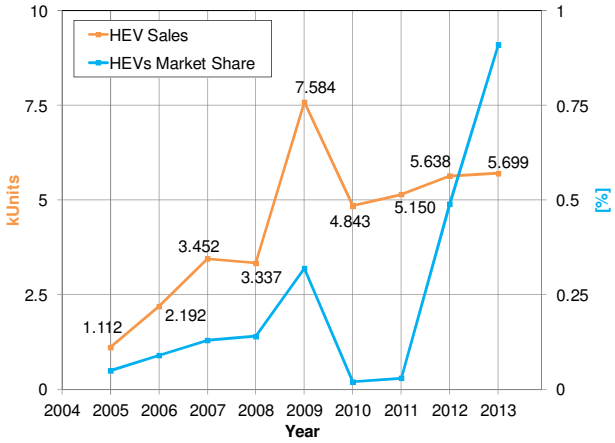


**Figure 3** *Number of units sold and market share for hybrid electric vehicles in Italy.*

In particular the above Figure 3 refers to both traditional and plug-in hybrid vehicles, which presents the interesting feature of recharging their battery pack directly from the main grid. The higher values of units sold for HEVs with respect to EVs is justified by lower cost of their battery pack and higher travel range. In fact, hybrid thermal-electric propulsion system can take advantage of high energy density and low refilling times generally related to the use of traditional oil based fuels. Nevertheless also in the case of HEVs the market penetration is still very low, reaching a maximum percentage value of about 1% with respect to the whole automotive market. On the other hand it is possible to observe a constant grow, in terms of units sold, of about 26%/Year from 2005 to 2013.

In order to compare the Italian automotive market related to electric mobility with other countries, Figure 4 reports the number of EVs sold and the market share of electric mobility, taking the year 2013 as reference, for different countries.

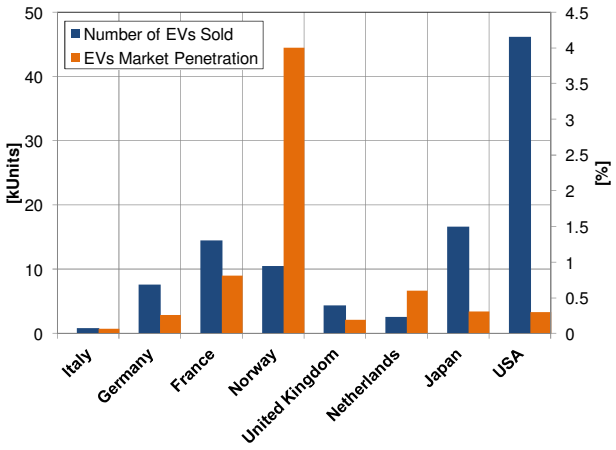


**Figure 4** *Number of EVs sold and market share – Comparison among different countries.*

From Figure 4 it is clear that, although market share of electric mobility can be still considered low, there are significant differences among the results reported for all the analyzed countries. In fact Japan and United States of America are characterized by a number of EVs sold 30 times higher in comparison with the Italian market and respectively represents the 28% and 26% of the worldwide EVs market.

On the other hand a different scenario can be observed for the values of market share analyzed for each country. In particular, Norway shows a market share of particular relevance reaching a value of about 3%. The positive trend of Norway can be justified considering the strong economic incentives, given by the government of this country, in order to support the adoption of EVs by private and corporate users. In fact the objective declared by the Norwegian government is to reach 50000 circulating road electric vehicles by the end of 2018. The incentives supporting this ambitious objective are mainly based on purchase VAT exemption, reduction of motorway tolls and possibility to access in limited traffic zones. Moreover the diffusion of electric vehicles in this country is further encouraged by the availability of a well-developed charging infrastructure, which is characterized by about 4000 charging points geographically dislocated in all the country.

The above considerations, related to different countries, evidence the effect of the availability of a proper charging infrastructure, supported by government incentives, on future large-scale adoption of electric and hybrid mobility [13].

### *1.2 Integration of PEVs and renewable energy sources in the smart grid scenario*

The considerations reported in the above paragraph have shown a slight but constant grow in the number of road electric and hybrid vehicles for all the analyzed countries. In fact these kinds of vehicles are now considered a good solution for urban mobility, reducing at the same time oil dependency and its related emissions in the earth atmosphere. Nevertheless a transition towards a clean road mobility system is strictly related to the proper integration of PEVs with actual electric power system. In particular, the existing electric infrastructures are not specifically designed to satisfy the increase in power demand related to a large-scale diffusion of this kind of vehicles. In fact simultaneous and uncontrolled PEVs charging operations are expected to directly affect the electric power distribution system, involving high power peak and overload capacity, with the consequent over-dimensioning of cables, power transformers and other components [14]. On the other hand, when the integration of a large-number of PEVs with the electric power system is well planned, the wide adoption of the electric mobility could add value to the main grid in terms of efficiency, performance and power quality [10].

In addition, in order to perform the vehicle charging operations without further environmental issues, which are directly related to traditional generation systems, the main grid is required to integrate a growing amount of distributed generating units, based on Renewable Energy Sources (RESs), such as solar, wind and sea waves [15]. Unfortunately RESs are generally considered unpredictable, in terms of generated power, since they are affected by both daily and seasonal changes in meteorological conditions, such as wind speed, solar radiation, temperature, etc. [16][17].

The above issues can be properly addressed in a smart-grid scenario, which consists in the integration, supervised by specific intelligent devices, of the existing electric power system with distributed generating units, stationary energy storage systems and electric mobility [18].

#### *1.2.1 The smart grid concept*

Nowadays the electric power system is mainly characterized by centralized power architecture where the electric energy production is demanded to high power generating units, generally based on the use of traditional fossil fuels. On the other hand, the growing amount of distributed energy generation systems, also affected

by natural power fluctuations of RESs, can not be faced with the existing power system architecture. In fact, in order to compensate RESs power fluctuations, the base-load production of power plants would require a proper regulation. Nevertheless, this regulation is quite difficult and involves unacceptable efficiency losses [19]. An alternative solution would be the disconnection from the main grid of part of intermediate load following generating units, with the disadvantage of a strong reduction in reliability of the electric power system. As a consequence, the solution, commonly adopted in the network management, is based on the disconnection of some distributed/renewable energy generation systems, with consequent economic and efficiency losses for the whole generation system [20].

For the above reasons a transaction towards new clean and distributed architecture integrated with stationary energy storage systems is becoming a key issue to be faced in the next years. In this regards Figure 5 reports a schematic comparison between the existing and new electric power system architecture.

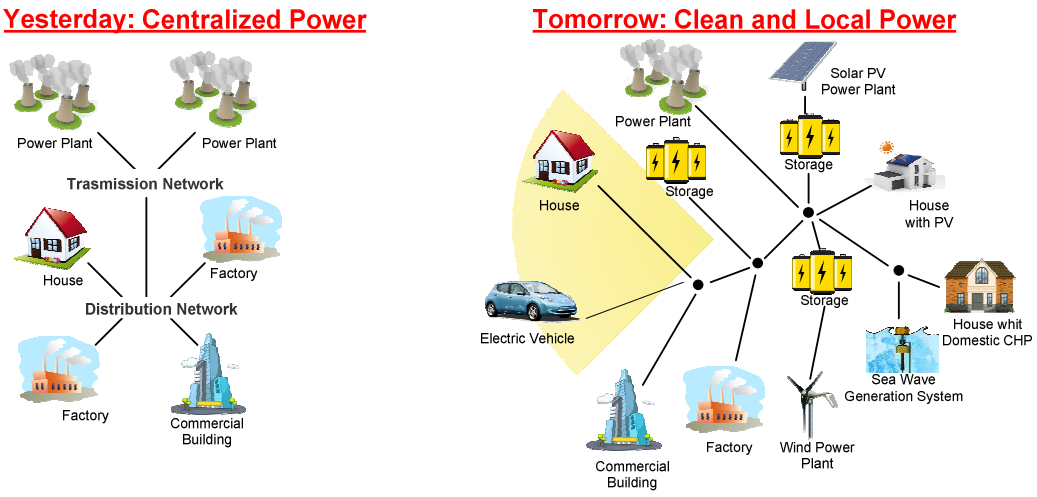


**Figure 5** *Comparison between existing and future electric power system architecture.*

The energy management in such distributed architecture becomes more complex and challenging, involving the control of active/passive loads, energy storage systems and low power unpredictable generating units. As a consequence the integration in the electric power system of intelligent devices, specifically devoted to energy control and metering, becomes an essential requirement to face this new scenario.

In this context, the smart grid concept can be considered as a new technology identified by the combination between Information & Communication Technology and power system engineering, which aims to obtain a flexible, efficient and reliable electric power system [18].

Following users and electrical power system needs a smart grid is designed to satisfy the following requirements [21]:

- *Intelligence*: the smart grid is characterized by "intelligent" sensors and control equipment, able to perform calculations, measures and to communicate with other devices.
- *Energy market oriented*: smart grid architecture allows active participation of users with real-time communication between the consumer and utility companies. These communications allow network operators to treat users as resources available in the daily management of the network, facilitating the movement of peak demand and the formulation of real-time pricing;
- *Open*: smart-grid architecture is conceived to accept energy coming from several sources supporting new technologies, new services and new markets.
- *Focused on quality*: The integration and management of stationary energy storage systems in combination with distributed generating units increases power quality avoiding voltage drops, peaks, disturbances and interruptions.
- *Robust*: the integration of intelligent device increase reliability of the whole grid.

It is clear that the transaction towards new electric power system architecture based on the adoption of the above concepts requires economic and technological effort. From this point of view an unexpected support can be represented by electric vehicles during their charging operations [9]. In fact, as described above, one of the most attracting features of the smart grid concept is the possibility to balance the power generation from unpredictable RESs. This objective can be reached through the proper management of stationary energy storage systems or controllable dispatch loads [22]. Nevertheless the large adoption of stationary energy storage systems involves high investment and maintenance costs, which have actually delayed the wide spread of renewable energy generation systems [18].In this context, PEV batteries, when connected to the main grid, can work as stationary energy storage systems, which smooth the surplus of electric power generated by RESs, through different charging schemes. Moreover they can also

feed the electric power back to the main grid, in supplying regulation and ancillary services through the Vehicle to Grid (V2G) schemes [23].

### *1.2.2 Vehicle to grid operations*

Electric and hybrid plug-in vehicles, when integrated in a smart grid scenario, can be considered both as dynamic loads, drawing energy from the main grid, and as stationary energy storage systems, supporting the main grid with ancillary services. This last operative condition is generally referred as Vehicle to Grid (V2G) operation. The V2G concept is based on the aggregation of a large number of EVs, on the base of specific control schemes, in order to support electric grid in regulation and management operations [24].

PEVs can support the main grid, realizing V2G operations, through bidirectional or unidirectional power flow management.

In the first case the electric power is supplied by the main grid, when the vehicle is on charge, and can be fed back, from the vehicle towards the main grid, in order to perform active participation in energy and ancillary services market. On the other hand in case of unidirectional power flow management, the electric power can be only supplied by the main grid toward the vehicles on charge. In this last case PEVs owners are enabled to participate in the energy market providing frequency and voltage regulation [25].

Bidirectional V2G system can support the grid with higher quality ancillary services in terms of voltage and frequency regulation playing also the role of efficient peak power and spinning reserves. Unfortunately, the need to involve extensive safety protection measures, such as anti-islanding protection, and the higher cost of power electronics related to bidirectional charging systems reduce the economic benefits of this mutual interaction between the grid and EVs [9]. Moreover the ancillary services supplied by a single vehicle are often negligible, in terms of available electric power and energy, with respects to the needs of the main electric grid, and might strongly affect the EV battery durability and owners' acceptance towards V2G operations.

In fact the continuous battery cycling required by V2G operations strongly affects the battery durability as a function of the depth of discharge of each cycle. In this regard Figure 6 reports the durability, in terms of number of cycles versus Depth of Discharge, for a $LiFePO_4$battery pack, which is a typical energy storage system used for automotive applications [26].As it is clear from Figure 6 the EVs

battery pack can support a high number of charging and discharging operations but only for very low values of depth of discharge. For this reason the contribution that a single vehicle can give to the main grid in terms of power supplied is further reduced.

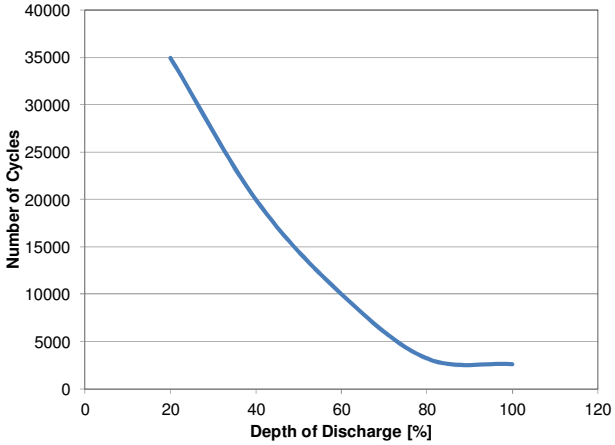


**Figure 6** *Number of Cycles vs Depth of Discharge for a LiFePO4 battery pack.*

Higher benefits can be surely obtained when PEVs are not considered as single entities and are grouped with an aggregation logic supplying high power bidirectional V2G services to the main grid.

### *1.2.3 V2G Aggregation Schemes*

In order to obtain a large scale adoption of V2G ancillary services, the requirements of both Grid System Operator (GSO) and vehicle owners need to be satisfied. In particular, on the operator side, availability and reliability of V2G operations are considered as fundamental features of these services, whereas vehicle owners would aspect to obtain a strong return from their investment in a vehicle technology, which support bidirectional V2G operations.

The above requirements can be reached with either direct or aggregative power and communication architecture [27].

The main scheme of a direct V2G architecture, also called deterministic architecture, is reported in Figure 7.

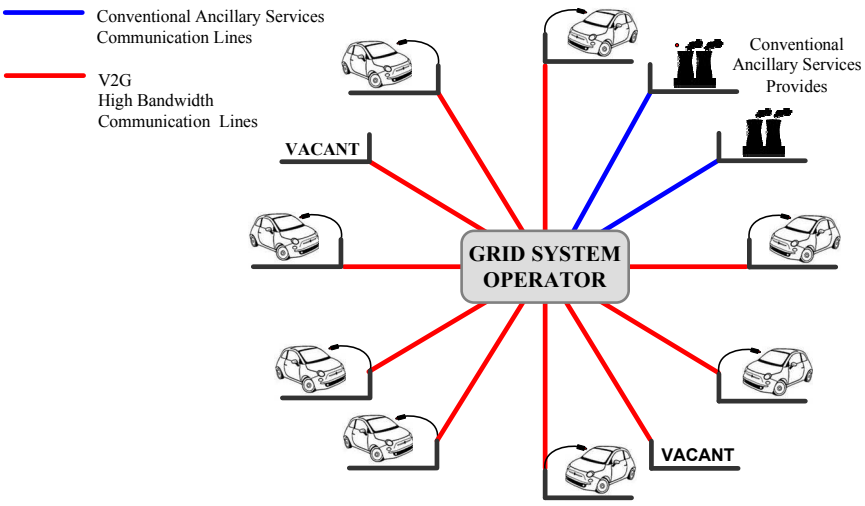


**Figure 7** *Main scheme of a direct V2G architecture.*

In particular this architecture is based on a direct communication scheme between the GSO and the vehicles on charge. In this way the EVs are autonomously controlled by the operator as single deterministic power sources, trough direct communication and power lines. Under deterministic power and communication scheme, the PEVs connected on charge can trade with the grid operator for ancillary services, whose availability ends when the vehicles leave the related charging point. The direct architecture represents a quite simple scheme for the management of V2G operations but it is strongly affected by recognized technological issues. These issues are mainly due to the absence of proper communication infrastructure able to manage the huge amount of measuring and control signals related to the interaction of the GSO with each vehicle on charge. In fact the interaction between the GSO and EVs, in direct scheme, is required to be based on high bandwidth communication lines because of the geographically distributed nature of V2G services. Moreover in long-term evaluations, based on different possible penetration scenarios [11], a high number of vehicles can be continuously engaged and disengaged from the grid. In this context the GSO is required to constantly update information about contract status, connection status, owner requirements and state-of-charge for each PEV.

The main scheme of aggregative indirect V2G architecture is reported in Figure 8.

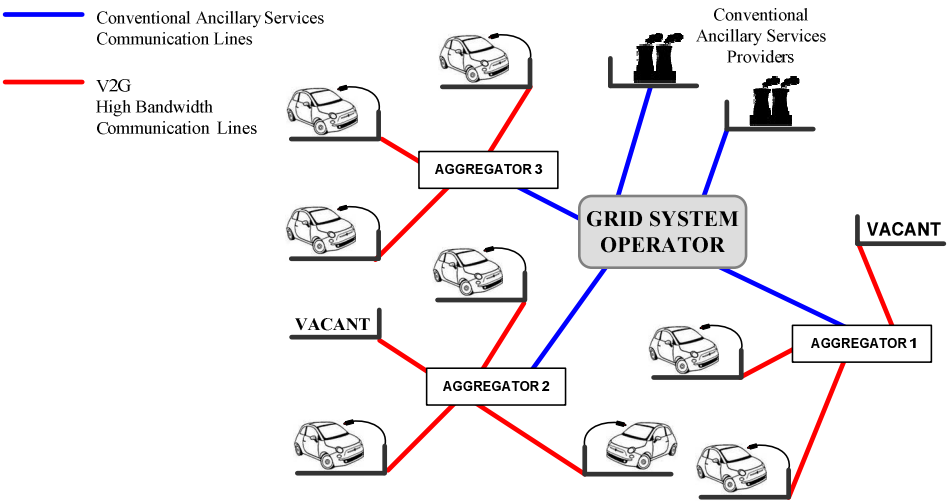


**Figure 8** *Main Scheme of Aggregative Indirect V2G Architecture.*

With this architecture PEVs are grouped and managed with aggregative logic and act as virtual power plants (VPPs) during V2G operations [18].In this context the role of the Aggregator is devoted to the management of a high number of charging vehicles on the base of the main grid operative conditions and requirements. In particular, the aggregator works as an intermediate service interposed between the GSO and groups of vehicles on charge. Following this power and communication scheme, the aggregator receives from the GSO specific requests for supplying ancillary services. Then, trough high bandwidth communication lines it enables and manages the V2G operations of different available vehicles. In this way the aggregator can supply the main grid with high power ancillary services at any time, whereas vehicle owners are free to choose when to connect/disconnect the vehicle from the specific charging point, following their specific habits.

The aggregative architecture presents different advantages with respect to the deterministic power and communication scheme. In fact the high number of vehicles, able to perform V2G operations and grouped under the same aggregation scheme, improves the reliability and availability of ancillary services provided by the aggregator. As a consequence, during its interaction with GSO, the aggregator can be considered as a conventional ancillary services provider, based on the same existing communication infrastructure. In fact, with the aggregative architecture, the GSO performs deterministic communications only with a reduced number of

aggregators rather than a high number of geographically distributed vehicles. On the other hand, the infrastructure supporting the communication between the aggregators and vehicles is strongly reduced with respect to the direct architecture, where the GSO is required to perform high bandwidth communications with each vehicle connected to the charging points.

For the above reasons the indirect aggregative architecture can be considered more modular and extensible, in comparison with the direct scheme, since it allows to support the increasing number of vehicles, performing V2G operations, with an increased number of aggregators[27][28].

### *1.2.4 PEVs charge in the smart grid scenario*

In the context of a smart grid scenario the smart charging of PEVs allows vehicle owners and GSO to schedule vehicle charging profiles in order to get technical and economic benefits. Following the aggregative power and communication scheme reported in the previous paragraph, also vehicle charging operations can be properly managed and optimized through the use of aggregators. In particular, the aggregator control can be performed on the vehicles either in a centralized or in a distributed framework [1].

The main scheme of a centralized control framework is reported in Figure 9 [29].

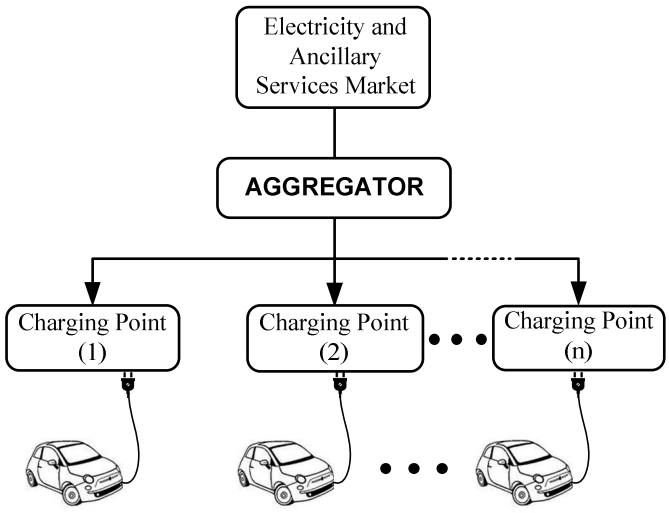


**Figure 9** *Main scheme of a centralized control framework.*

In this case, the aggregator directly manages the charging operations of all the vehicles connected to the charging points, which are grouped under its responsibility. Moreover the aggregator controls also other entities, such as charging post managers, which are in charge of PEVs parks management. In this control framework, the aggregator evaluates proper algorithms, based on the collection of data related to status and owner's preferences for each charging vehicle, in order to achieve specific objectives. These objectives are mainly focused on the maximization of aggregator profits and the optimization of charging operations in terms of cost and grid impacts [25]. As a consequence, with this configuration, the aggregator is also responsible for the participation of the vehicles in the electricity and ancillary services market.

The main scheme of a distributed control framework is reported in Figure 10 [29].

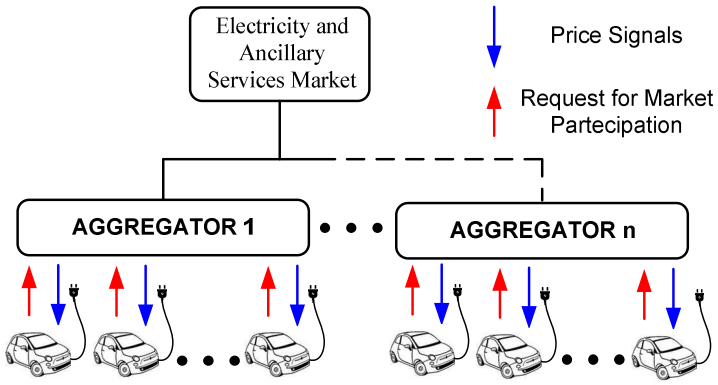


**Figure 10** *Main scheme of a distributed control framework.*

In this case the decisions of charging or V2G operations are committed to each connected vehicle. For this reason, with distributed control framework, each vehicle is required to be equipped with intelligent devices called Vehicle Management Systems (VMS). Although in this case the availability of the vehicle, in supporting aggregator needs, may depend on VMS and owners' preferences, different strategies can be adopted to realize an almost predictable load/generation profile. These strategies are mainly aimed to cost reduction for the customers, during their charging operations. In particular, as reported in Figure 10, the aggregator can send information about the electricity price to each vehicle. Then each vehicle, through specific algorithms running on its VMS, performs evaluations aimed to optimize the cost of charge, taking into account owner's

preferences but without exchanging this information with other physical or virtual entities. Following the same operational scheme, each VMS can send to the aggregator specific request for the participation in V2G operations [1].

In addition, distributed control framework can be aimed also to other specific objectives, such as reduction of air pollution in green areas, reduction of charging times, maximization of V2G operations etc... For this reason the management of distributed control framework needs to be performed taking into account different objectives, which may depends on geographical, economic and technological reasons. One of the most common approaches to deal with such a complex distributed system is referred as Multi Agent System (MAS) [30]. MAS can be considered as a set of more intelligent entities, called Agent, which cooperate and communicate each other dividing complex computational problems into more simple sub-problems. Following literature definition [31], an agent is characterized by: autonomy in taking decision without continuous user feedback; communication ability, in order to interact with other agents; ability to start its own action to follow a specific goal; ability to receive external information and rapidly respond to changes.

In this scenario each vehicle on charge has its own reference agent with its own objective, according to its status and to the status of the other agent working in the same MAS.

### *Conclusions*

This chapter, starting from a market analysis of the Italian and International automotive sectors, has shown the main technical bottlenecks and enabling factors for a large scale adoption of PEVs. From the reported analysis it results that although the market share of PEVs is still very low, a constant grow in the number of sales related to this kind vehicles can be observed. This is mainly justified by the availability on the market of a new generation of electric vehicles characterized by high performance and innovative design. The comparison among different countries has evidenced that national incentives and large-scale development of charging infrastructure can be considered as relevant enabling factors for the diffusion of electric vehicles.

In addition this chapter has introduced the concept of smart grid with specific focus on its role in the intelligent integration of PEVs with renewable energy sources and stationary energy storage systems. In the smart grid context different

aggregation, communication and control architecture have been described evidencing the real advantage of using distributed aggregative schemes based on Multi-Agent systems for the smart integration of PEVs aimed to optimize V2G and charging operations.

# **Chapter 2.** Charging infrastructure for electric and plug-in hybrid vehicles

***Introduction***

As described in the above chapter, the development of a proper charging infrastructure, both for public and for private use, is considered one of the key enabling factors for the wide spread of PEVs. In comparison with the refueling facilities for traditional oil based road vehicles, charging infrastructures for PEVs are generally characterized by a large variety of topologies, which can be mainly classified on the base of the rated electric power and maximum charging times. In particular residential or working place charging devices are generally related to low power charging operations and can be considered suitable for the slow charge of the vehicle when it is parked for a long period of time. On the other hand fast charging operations are required to enable the use of PEV also for long travel distances. In this case, high power devices can be considered in order to charge the vehicle in less than 30 minutes. The impact that these kinds of operations may have on the electric power system needs to be properly taken into account in order to avoid unexpected overload conditions for the main grid. This issue can be properly addressed in a smart grid scenario taking advantage of distributed stationary energy storage systems, which support the main grid during fast charging operations.

This chapter starts with an analysis of the existing charging infrastructure considering the relationship between the diffusion of PEVs on the local market and the development of the national charging infrastructure. Then the different PEV charging modes considered by the SAEJ1772 standard are described with detailed information on DC charging modes and related connectors. The chapter continues with a description of possible charging architecture specifying advantages and drawbacks related to AC and DC bus configurations. In this context particular focus is given to buffered architecture, which is proposed in order to mitigate the impact on the main grid of the fast charging operations. The chapter ends with a detailed description of distributed buffered architecture based on the use of multilevel converters.

### *2.1 Analysis of charging infrastructure for electric and plug-in hybrid vehicles*

Nowadays the Italian charging infrastructure for electric and plug-in hybrid vehicles is characterized by 642 public charging points, which are dislocated in 74 provinces. The geographic distribution of public charging points in Italy is reported in Figure 11 [32].


**Figure 11** *Geographic distribution of public charging points in Italy.*

Although an average value of about 10 charging points for each province has been evaluated, it is possible to observe that many Italian cities are still equipped with only one charging point. Moreover the 60% of charging points are located in Florence, Rome and Milan, which in the past have taken advantage of pilot projects supporting the diffusion of charging infrastructure. In this regard Figure 12 shows the first ten Italian provinces in terms of number of charging points. It is important to observe that 145 of the 642 charging points are based on the use of renewable energy sources, giving in this way a further contribution to the reduction of pollutant and greenhouse gases emissions. In particular Pisa and Rome are the cities with the highest number of this kind of charging points.

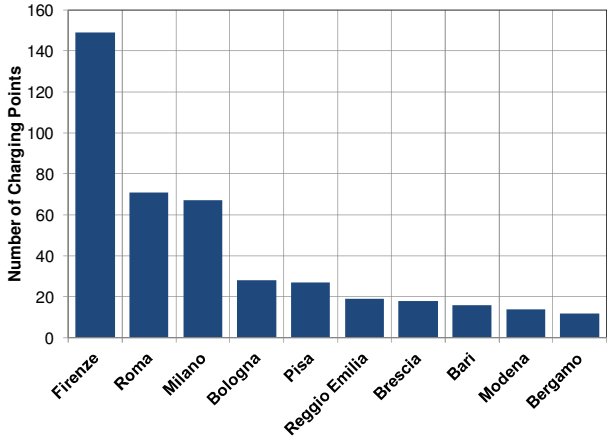


**Figure 12** *Number of charging points for the first ten Italian provinces.*

Taking into account the worldwide scenario, Figure 13 reports a comparison among different countries in terms of number of slow and fast charging points [33].

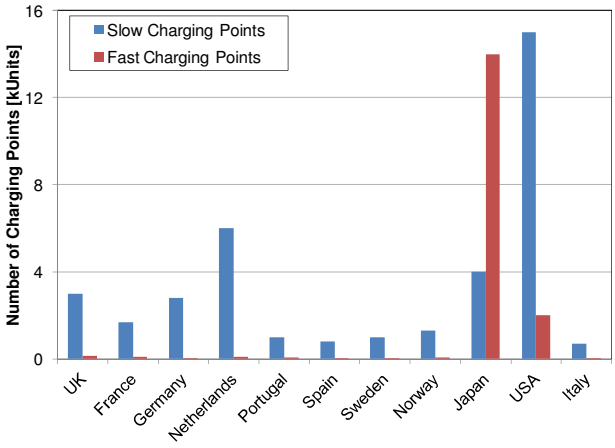


**Figure 13** *Number of charging points – comparison among different countries.*

From the reported comparison it is clear that the diffusion on the market of PEVs, evaluated in the first chapter, is strictly related to the development of a proper charging infrastructure. Moreover many countries are equipped for the main part of low power public charging points, which are related to slow charging operations. From this point of view, the only exception is represented by Japan, where the CHAdeMO (CHArge de MOve) consortium has given financial support to the diffusion of high power fast charging stations.

From the above considerations it is clear that the development of charging infrastructure is still very low, in the most of the country, and in many cases the

adoption of low power charging infrastructure has affected the diffusion on the market of PEVs both for private and for corporate use.

### *2.2 PEV Charging Modes*

The proper design of a charging infrastructure pursues the main objective of supporting PEV owners both with low power charging operations, related to short daily travel range, and with high power fast charging operations, which are required in order to satisfy longer travel range.

On the base of the rated power of the charging point and of reachable refilling times, different PEV charging levels can be defined. These levels have been classified by the SAEJ1772 and associated to slow and fast charging operations. A brief summary of these levels is reported in Table 1 [18] [34].

| **Level** | **Charging Voltage [*V*]** | **Maximum Current [*A*]** | **Maximum Power [k*W*]** | **Charging Time** | **Charger Location** | **Voltage Supply** |
|---|---|---|---|---|---|---|
| AC Level 1 | 120 ÷ 230 AC | 16 | 2 | 7 ÷ 17 *h* | On Board | Single-phase |
| AC Level 2 | 230 ÷ 400 AC | 80 | 20 | 1.5 ÷ 7 *h* | On Board | Single/tri-phase |
| DC Level 1 | 200 ÷ 500 DC | 80 | 40 | 22 *min* ÷ 1.2 *h* | Off Board | Tri-phase |
| DC Level 2 | 200 ÷ 500 DC | 200 | 100 | 10 *min* ÷ 20 *min* | Off Board | Tri-phase |
| DC Level 3 | 200 ÷ 600 DC | 400 | 240 | < 10 *min* | Off Board | Tri-phase |

**Table 1** *AC/DC charging levels reported in the SAE J1772 standard.*

AC level 1 charging operations generally refer to the connection of PEVs to a charging point supplied by a single phase AC line not exceeding 230 *V* AC. This charging mode is generally performed by means of national plug and socket system not exceeding 16 *A* depending on the specific country and standardization. The low power charging operations related to this mode are the slowest and can be considered suitable only for the recharging of vehicles during the night or when vehicles are parked for a long time. On the other hand this mode ensures low costs for the vehicle owners and low power requirement from the main grid. In addition, in this case, no specific charging equipment is required but only protective earth conductors have to be considered for safety reasons [35].

AC level 2 charging operations refer to the connection of PEV to high power charging points, supplied by single-phase or tri-phase AC network. In this case the maximum charging current does not exceed 80 *A*. This charging mode is typical of public charging stations and is generally supplied by tri-phase AC voltage at 50/60 *Hz*. It is also called 'semi-fast' charging solution since the PEV battery pack can be charged in few hours when the driver is at work or during every day activities. In this case, the charging equipment is more complex since connectors with a group of control and signal pins are required for both the vehicle and socket side of the cable. Actually the charging power of this level is limited by the fact that the AC/DC conversion is committed to the on board charger, whose rated power is affected by vehicle size and weight requirements [35].

DC charging Levels 1÷3 have been initially developed by CHAdeMO consortium and are characterized by the use of off-board DC charging stations. In this case the charging station is permanently connected to the three-phase AC network and integrates the power electronics devoted to the conversion from AC to DC voltage, which is required for the supply of PEV battery packs. In this case smart control systems are integrated both on board and in the DC charging station, which is required to adapt voltage and current profiles to the specific vehicle battery pack requirements. In fact in this case the whole charging procedure is managed through the continuous communication between the charging station and the BMS of the vehicle battery pack. Typical PEV refilling times of DC charging levels are in a range from 20 to 30 minutes. Actually the charging power is limited in many cases by the maximum allowable current of 125 *A* and voltage of 500 *V* of the existing CHAdeMO standard connector [8]. Combining high power converters with the latest battery technologies this charging mode could allow a recharge from 0 to 80% of battery SoC in less than 5 minutes. This last type of recharge is also referred as ultra-fast charge [8].

Fast charging operations are considered an essential step in order to obtain a wide diffusion on the market of PEVs. Nevertheless there is still a great debate on how to get a universal standard on fast charging connectors. In this regard two different technical solutions have obtained a large acceptance by PEV and charging stations manufacturers. A first solution which has gained a remarkable diffusion among Japanese vehicle manufacturer is CHAdeMO connector, whose picture is reported in Figure 14. The CHAdeMO standard has been developed by the CHAdeMO association [36], which involves different Japanese companies

operating in the automotive (such as Nissan, Mitsubishi and Toyota) and power electronics filed. This connector is specifically designed to supply vehicle battery packs with high values of DC voltage and current.

**Figure 14** *Picture of the CHAdeMO connector.*

The most relevant drawback of the CHAdeMO standard is that it is generally related to a vehicle inlet, which supports only DC charging operations. For this reason an additional AC inlet has to be installed on the vehicle in order to support slow AC level charging procedure. As a consequence CHAdeMO standard has been adopted only by Japanese car manufacturers whereas American and European companies have refused the adoption of this standard [37].

In order to solve the main issues related to CHAdeMO standard, another connector have found a wide diffusion in the automotive sector. This connector, whose picture is reported in Figure 15, has been realized on the base of collaboration among European and American automotive manufacturers and the Society of Automotive Engineers (SAE). For this reason it is also referred with the name of SAE combo connector [18]. In this case AC and DC pins are integrated on the same connector. As a consequence AC single phase (AC level 1), AC tri-phase (AC level 2) and DC (DC level 1 ÷ 3) charging operations can be performed trough SAE Combo connector [37].

**Figure 15** *Picture of the SAE combo connector.*

Following the above charging levels and mode it is clear that the charging power delivered by the main grid to charge the vehicle, is strictly related to the rated power of the on-board/off-board battery charger and to the performance of PEV storage systems.

### *2.3 AC and DC charging architecture*

In the smart grid scenario, different micro-grid architecture can be proposed with the aim of enabling the energy sharing among stationary energy storage systems, PEVs and renewable energy sources.

In particular two different configurations, mainly based on the use of either AC bus or DC bus, are generally suggested in the literature [7].

The use of AC bus architecture is supported by the fact that the existing transmission and distribution infrastructures have been designed to work with AC voltage. As a consequence the great part of the electric loads both for domestic and industrial appliance are supplied by AC voltage. The main scheme of a charging architecture based on the use of AC bus is reported in Figure 16 [38]. In this case the electric power exchange among the vehicles on charge and renewable energy sources is managed by controlling each bidirectional AC/DC converter. In addition also vehicle to grid operations are obtained through the direct control on the PEV battery chargers.

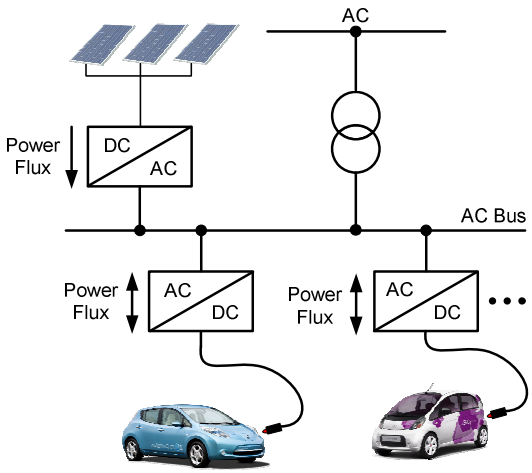


**Figure 16** *PEV charging architecture based on AC Bus.*

On the other hand, as mentioned in the previous chapter, the new electric power system scenario is characterized by distributed DC electric loads, represented by the PEVs on charge, generation units, mainly based on renewable energy sources, and stationary energy storage systems. This new scenario, supported also by the growing diffusion of DC electronic equipment for domestic and office appliance, justifies research and technical interest towards the use of DC architecture. As matter of fact PEV storage systems are required to be recharged using DC voltage, involving in the most of the case the connection to AC infrastructures trough low efficiency AC/DC conversion stages. In addition, also distributed electric generation units, based on Renewable Energy Sources (RESs), are generally realised in DC. In this case, in order to tie with the AC bus, the generated voltage would be required to be converted in AC and then probably converted again to supply DC electronic equipment or PEV battery pack. This DC-AC-DC conversion strongly affects the electric energy generation from RESs with high efficiency losses. The above issues can be properly addressed with the DC bus architecture reported in Figure 17 [38].

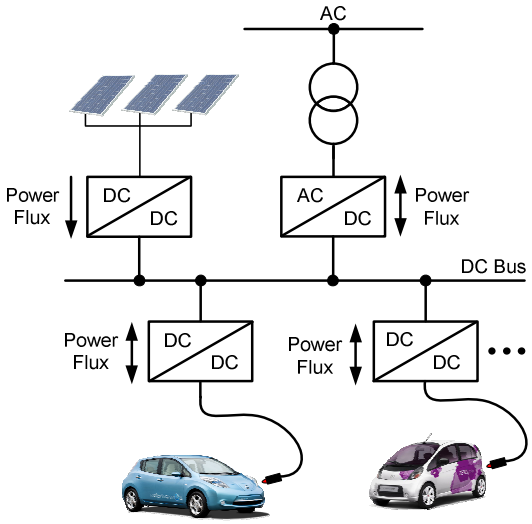


**Figure 17** *PEV Charging Architecture with DC Bus.*

With the above architecture the DC bus is realized by means of a high efficiency AC/DC converter, also referred as grid-tied converter [7]. The vehicles and renewable energy sources are connected to the DC bus trough high efficiency DC/DC converters. In this way it is possible to take advantage of high efficiency DC/DC voltage conversions, avoiding also the double conversion losses (DC-AC-DC) related to RESs. The energy exchange on the DC bus is managed trough the proper control of the DC/DC converters related to PEVs and RESs, whereas V2G operations are obtained through the AC/DC grid tied converter. Other advantages of DC bus architecture are related to the facts that the synchronization of distributed generators is not necessary and the power quality is not affected by inrush current, single phase loads and generators. Moreover, it can be evaluated that the use of this architecture reduces the whole conversion losses from about 32% to less than 10% [39]. Nevertheless also DC architecture presents some disadvantages in terms of costs mainly related to lack of expertise on this kind of configuration.

### *2.4 DC charging architecture based on energy storage buffers*

One of the main issues for the large acceptance of PEVs in the private automotive market is mainly related to their charging times, which are considered too high in comparison with traditional oil based road vehicles. This comparison can be better analyzed by an evaluation of the vehicle Autonomy Flowrate (AF).

The AF term can be defined as the increase of the distance covered by the vehicle for each minute of recharge and can be expressed through equation ( 1 ).

$$AF = \frac{C_R}{T_C} A_c \qquad (1)$$

Where, $C_R$,is the charging rate, $T_C$is the tank or battery capacity and $A_C$ is the evaluated vehicle autonomy after a complete refilling/charging procedure.

A comparison between a small city diesel car and an electric vehicle is reported in [8], in terms of AF, considering respectively a tank capacity of 45 *l* and a battery pack capacity of 24 *kWh*. It results that, with the existing charging technology, the electric vehicle presents an AF of 4 *km/charging minute*, which is about 180 times lower than the case of the diesel car. These results can be justified taking into account the differences between the two vehicles in terms of vehicle autonomy after a complete recharge, $A_C$, and in charging rate, $C_R$. In particular, from simple calculations, it can be evaluated that PEVs should be equipped with a battery capacity of about 135 *kWh*, supported by a charging power of 6.3 *MW*, in order to reach the same AF values of the traditional oil based cars. The above values are not considered reachable in the short term with the existing energy storage and power electronics technologies [8].

As a matter of fact the traditional oil based vehicle autonomy, which can be evaluated as about 800 km, should not be taken into account for the above evaluations. In fact, no vehicle owner is expected to drive for 800 *km* without any intermediate stop. In addition the daily travel range of road vehicles has been evaluated as less than 50 *km* in 80% of the cases, as their use is related for the great part to urban areas [6]. In these cases low power charging operations can be considered suitable for end users, since the refilling of vehicle battery packs during the night, in 8÷10 hours, ensures a travel range from 100 to 150 *km* during the daylight. A feasible solution to obtain longer traveling distances would require frequent charging stations along the road, able to supply a significant amount of power to the vehicle battery packs. In this way, although PEV autonomy is lower than the case of oil-based fuel cars, their recharging time could be reduced to a 'fuel stop'- equivalent time.

In order to pursue the objective of a strong reduction in charging time, the main issues are related to the electricity distribution system, which is required to supply high power peaks during the ultra-fast charging operations, especially when fleets of vehicles need to be charged in few minutes at the same time. To support

this consideration, Figure 18 reports the electric power from the main grid involved in the charging operations of three different types of electric vehicles, characterized by battery packs of different in size, from 0 to 80% of their SoC.

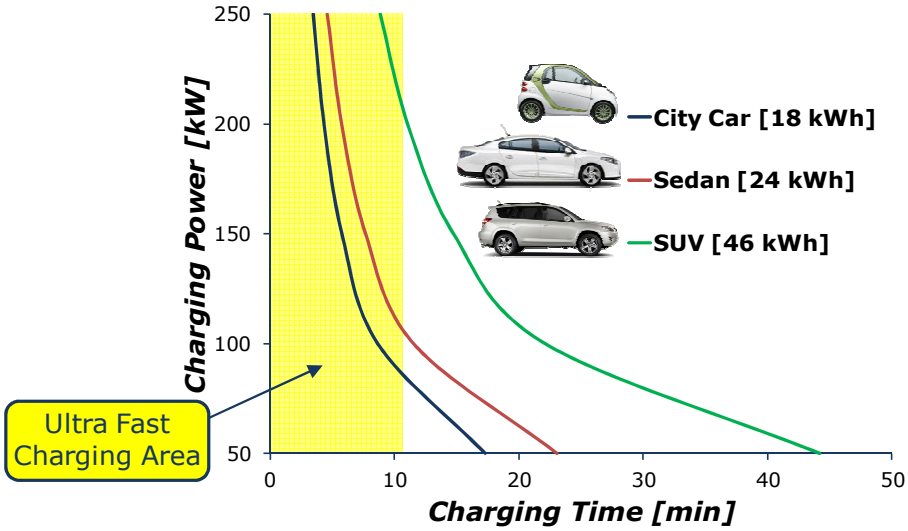


**Figure 18** *Power Requirement of the Ultra-Fast Charge.*

From the above figure it is clear that to obtain a charging time lower than 10 *mins*, for the three considered typologies of vehicles, an amount of electric power from 100 to more than 250 *kW* needs to be provided from the main grid to the charging point. As a matter of fact the main grid is not properly dimensioned to support these operative conditions, which would involve an over-dimensioning of cables, power transformers, devices, etc.. As a consequence in the design of PEV charging architecture the impact of the fast and ultra-fast charging operations needs to be properly taken into account.

The above issues can be properly addressed by using specific DC charging architecture based on stationary energy storage systems, which act as a buffer and support the electric power coming from the main grid during the charging operations of PEVs. This specific DC Bus architecture has been analyzed from theoretical point of view in different papers [8][7][38] and is also referred as buffered architecture. The main power scheme of this architecture is reported in Figure 19.

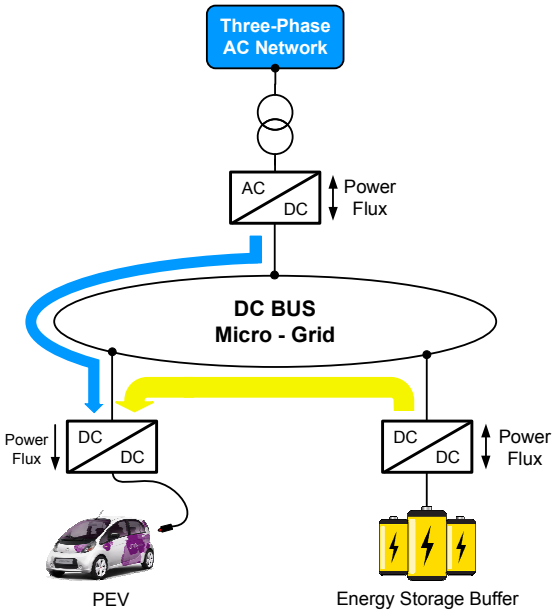


**Figure 19** *Main scheme of charging architecture with energy storage buffer.*

In particular the buffered architecture is characterized by two conversion stages obtained through AC/DC, also referred as grid-tied converter, and DC/DC converters. In this case the electric power required to perform the fast charging operations of PEVs is composed by two terms. The first term of power is represented by the flux coming from the main grid, which is represented in the above figure by the thin blue arrow and supply the DC micro-grid through the AC/DC converter. The second one is the power flux coming from the stationary energy storage buffer, which is represented in the same figure by the thick yellow arrow and goes through the DC/DC converter. As a consequence, following different designing criteria, the AC/DC grid tie converter can be conveniently and efficiently downsized in comparison with the actual power needed to recharge PEVs. In fact, the functions of the grid tie converter are limited to low power operations performed during either the low power buffering phase, when the energy storage buffer is charged by the main grid, or the fast charging of the vehicle, supported by energy storage buffer. It is clear that in this case the rated power of the grid-tied converter is affected only by the charging rate required for the buffering phase. On the other hand the power flux coming from the energy storage buffer gives the highest contribution of electric power during PEV charging

operations. In this case the proper design of the energy storage buffer is particularly relevant since the related battery pack is required to perform high discharging rates, in order to supply the DC bus with high values of electric power during the fast charging operations. In addition the buffer battery pack needs to be characterized by high performance in terms of durability, since it has to support the main grid during a high number of charging operations. As an example, for the fast charging operation of a 16 *kWh* battery pack, the evaluation reported in [8] considers a 460 *V* - 134 *Ah* $LiFePO_4$ energy storage buffer. In this case the use of the $LiFePO_4$ chemistry is justified by the fact that these batteries are characterized by high discharging rates, up to 10 C, and a high number of cycle life, up to 3000.

### *2.5 DC charging architecture based on Multilevel Converters (MCs)*

Nowadays, Multilevel Converters (MCs) are gaining more and more attention for their use in industrial and research applications. This is mainly due to the possibility of modular power architecture to take advantage of high number of voltage conversion levels. In this way it is possible to strongly reduce the harmonic distortion of the output voltage with positive consequences on dimensioning of filters. Further benefits related to this kind of conversion architecture are mainly identified by the reduction of power semiconductor losses and the higher level of modularity and reliability in comparison with traditional power conversion schemes [40][41].

The use of MCs was initially focused on the AC drive sector. However, encouraged by the above mentioned advantages, these devices have found a rapid spread also for different applications. In particular MCs can be considered particularly suitable for the integration of electrochemical energy storage systems, since batteries or super-capacitors can be used as distributed DC sources, supporting cascaded H-Bridge converter architecture [42].

#### *2.5.1 Background*

MC topologies are generally based on the cascaded connection of a large number of Sub-Modules (SMs). These SMs are generally electrically connected in series and are grouped in arms. These arms, also referred as branches, can be connected in different configurations on the base of the specific topology. In this regards Figure 20 represents two possible configurations related to single phase/single phase or single phase/DC (a) and tri-phase/single phase or tri-

phase/DC (b) conversion architecture. The specific AC or DC voltage conversion depends on the SM topology [40].

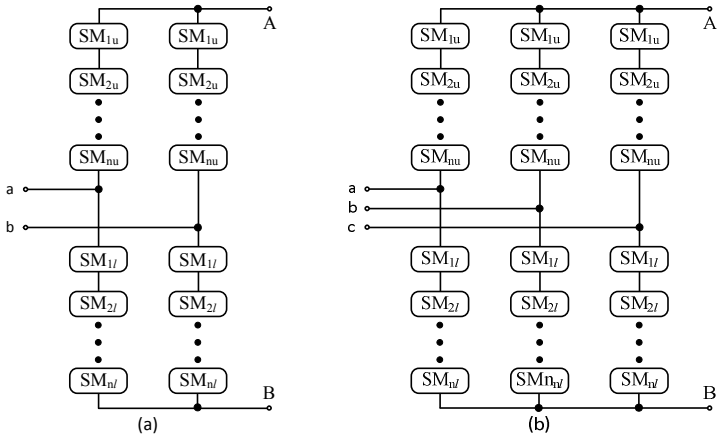


**Figure 20** *MMC topologies for single phase/single phase or single phase/DC (a) and tri-phase/single phase or tri-phase/DC (b) voltage conversion.*

Different SM topologies have been proposed in the literature on the base of their specific reference application. The most common presented topologies are related to the full-bridge and half-bridge configuration respectively represented in Figure 21(a) and Figure 21 (b) [40]. As clear from the reported schemes, with the half bridge SM (b), only null or positive values can be obtained on the arm side. For this reason this kind of configuration can be considered suitable only for the connection of the MC to a DC source. On the other hand, with full bridge topologies (a), it is possible to obtain positive, negative and null values of voltage. As a consequence, this last configuration can be used for the connection of MMCs both to AC and to DC systems.

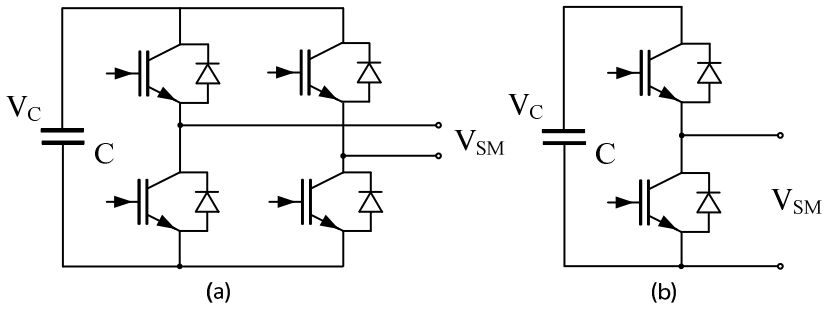


**Figure 21** *Full Bridge (a) and Half Bridge (b) Sub-Module Topologies.*

One of the drawbacks of the full-bridge configuration is related to the higher number of components, with respect to the case of the half bridge, with the consequent increase in the cost of the whole system.

### *2.5.2 Integration of energy storage systems with multilevel converters*

The integration of energy storage systems is generally performed by means of a cascaded H-bridge converter, whose main scheme is reported in Figure 22 [43]. In particular, this tri-phase architecture is based on a series of different SMs connected to single storage elements realizing a specific Storage Sub-Module (SSM). In this way each SSM can be properly controlled in order to overcome balancing issues related to the difference in voltage values of the energy storage units [44].

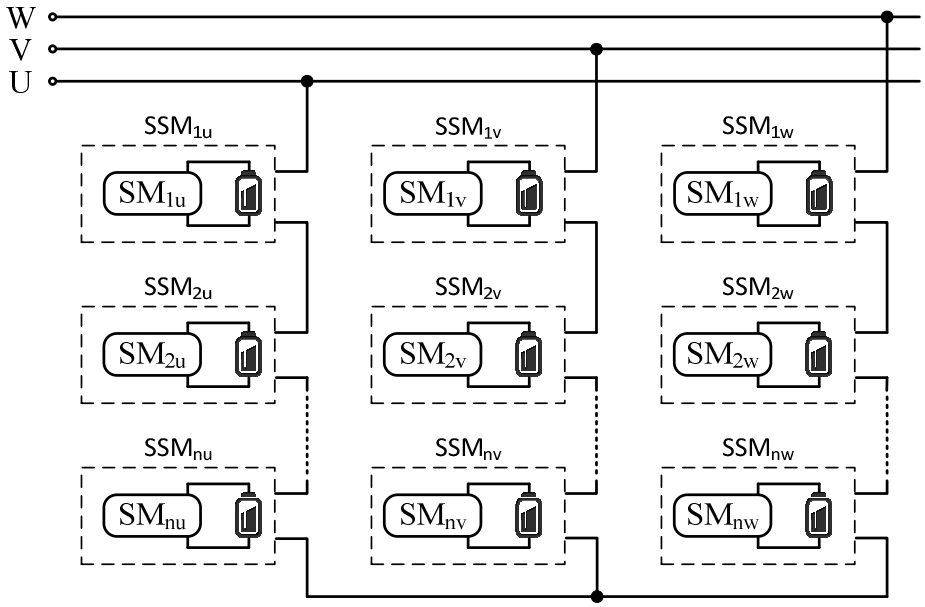


**Figure 22** *Main scheme of a tri-phase cascaded H-bridge converter.*

For the reasons explained in the previous sub-paragraph, the interaction between single phase or tri-phase AC grid and energy storage systems can be managed by using full bridge SM topologies. In this regard the energy storage unit is generally connected to the SM following one of the configurations reported in Figure 23.

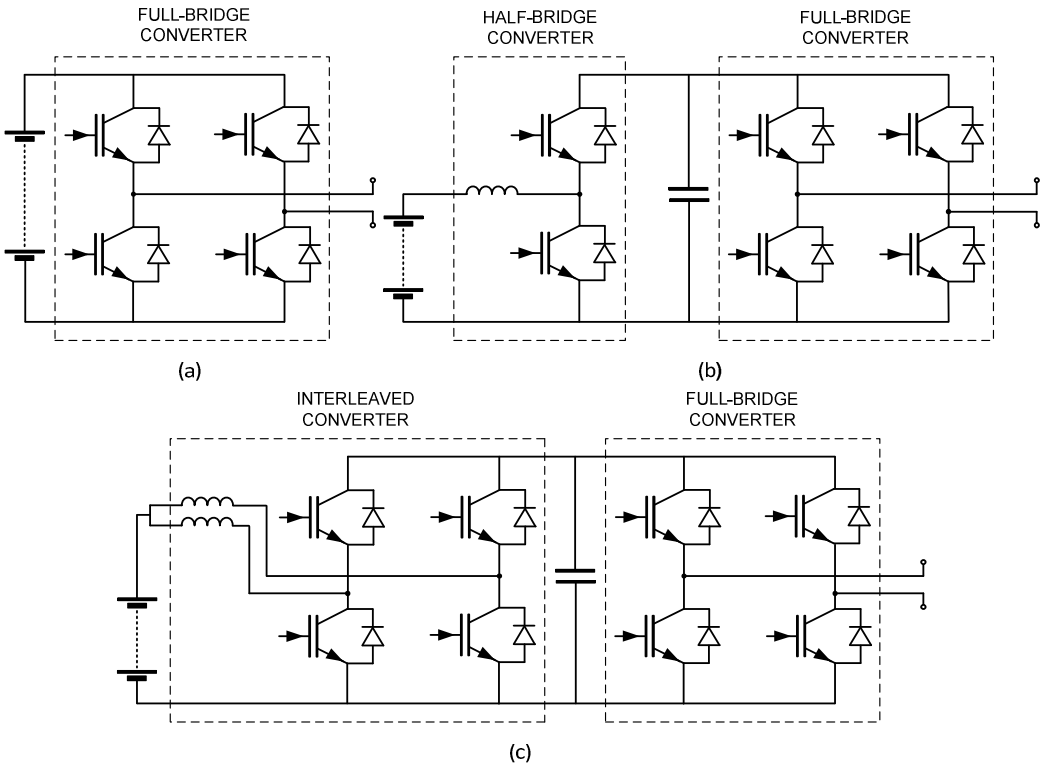


**Figure 23** *SM topologies for the integration of energy storage units.*

In particular in the configuration reported in Figure 23 a, the storage unit is directly connected to the H-Bridge converter. With this configuration, the SM controls both the AC/DC voltage conversion and the charging/discharging procedures of the related storage unit. The second configuration is based on a double-stage conversion scheme (b). In this case the charging/discharging operations of the storage unit are properly controlled by means of a half bridge DC/DC converter. This converter also allows decoupling the storage unit from the DC-Link of the H-bridge converter, which can performs in this way a better modulation of the AC signal. The third configuration reported (c) is similar to the second case with the only difference that in this case an interleaved boost converter is used on the energy storage side, in order to perform a reduction in the inductor current ripple [42].

### *2.5.3 Integration of multilevel converters and energy storage buffers for fast charging operations*

On the base of the topics introduced in the above sub-paragraphs, an evolution of the buffered architecture can be considered. In fact fast charging operations of PEVs, supported by energy storage buffer can be obtained by means of a distributed power architecture based on the use of multilevel converters integrating energy storage units.

Actually similar schemes have been proposed in the literature also for different applications taking advantage of the benefits related to the use of MCs [45][46].

In [47] the presented architecture is based on the configuration, reported in Figure 24, based on Cascaded H-Bridge (CHB) multilevel converter with SSM integrating energy storage units and full bridge isolated DC/DC converters. In this case, multiple DC conversion stages are obtained through a series of modular AC/DC bidirectional converters, connected with energy storage units. The outputs of the different SSM, working on a single branch, are connected in parallel in order to supply the PEVs with high charging power. This charging power is provided by the main grid supported by energy storage units, which work as power buffer trough the proper control of each SSM [48].

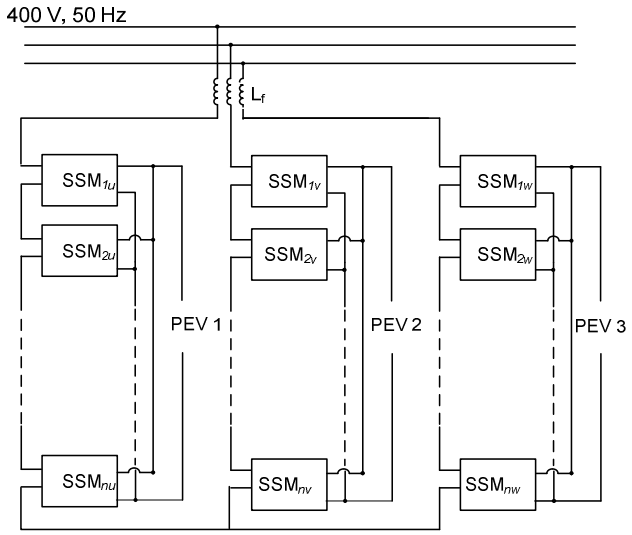


**Figure 24** *Fast charging architecture based on MCs and energy storage buffer.*

The main power scheme of the single SSM is reported in Figure 25.

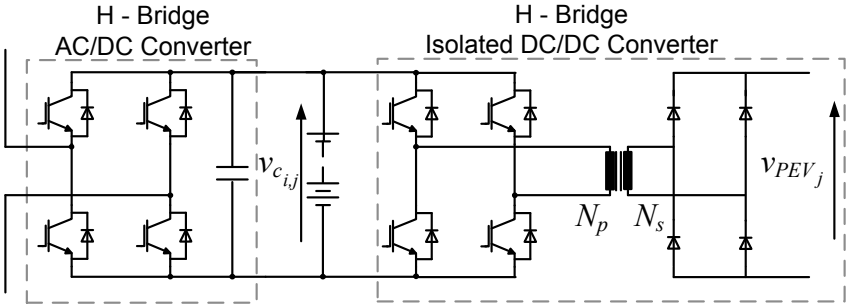


**Figure 25** *main power scheme of the single module integrating energy storage unit.*

In particular, $v_{ci,j}$, is the voltage related to the storage unit of the $SSM_i$ on the branch j, whereas $v_{PEVj}$ represents the battery pack voltage related to the vehicle on charge connected to the branch j. Each single SSM can be properly controlled in order to solve different functions. In particular the H-Bridge AC/DC converter can be used for low power charging and voltage balancing procedures of the energy storage units. Moreover it is also responsible for the management of the amount of electric power coming from the main grid during fast charging operations. The energy storage units can be connected to the DC link through a direct passive interface or an indirect active interface in order to reduce power fluctuations and increase the lifetime of the modules [48]. The charging operations of PEVs are managed through the control of the H-Bridge isolated DC/DC converter

Among storage technologies, different kinds of solutions can be investigated mainly based on different chemistry of super-capacitors and batteries. In [47], for the specific application $LiFePO_4$ storage units have been taken in consideration for their suitable characteristics. In fact this kinds of battery present very flat voltage charging/discharging curve, in a wide range of SoC, and good charging/discharging rates.

### *2.5.4 Main control scheme*

The main control scheme of the architecture presented in the above sub-paragraph is based on the hierarchical strategy reported in Figure 26 [46][47].

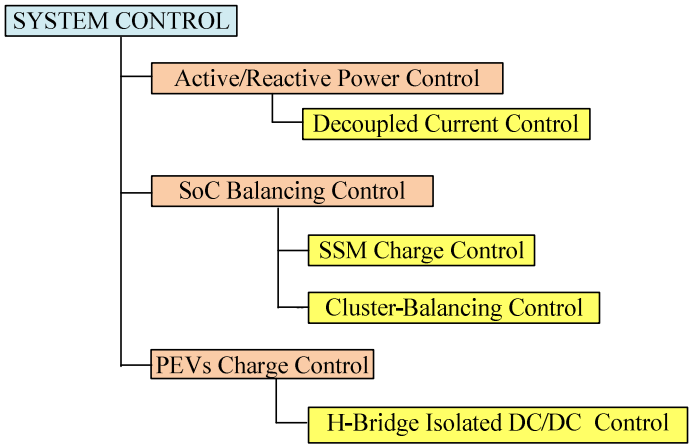


**Figure 26** *Main control scheme of a distributed buffer.*

As it is clear from the above scheme, the suggested control strategy is mainly based on the active/reactive power control, SoC balancing control, for each branch and among the SSM grouped on a single branch, and PEVs charging operation control.

*Decoupled Current Control Method*

The first control is focused on the management of the energy fluxes exchanged between the SSMs and the main grid. In this case the proposed control is aimed to perform an independent active and reactive power management by means of decoupled current method.

The main operative scheme of the decoupled current control method is reported in Figure 27.

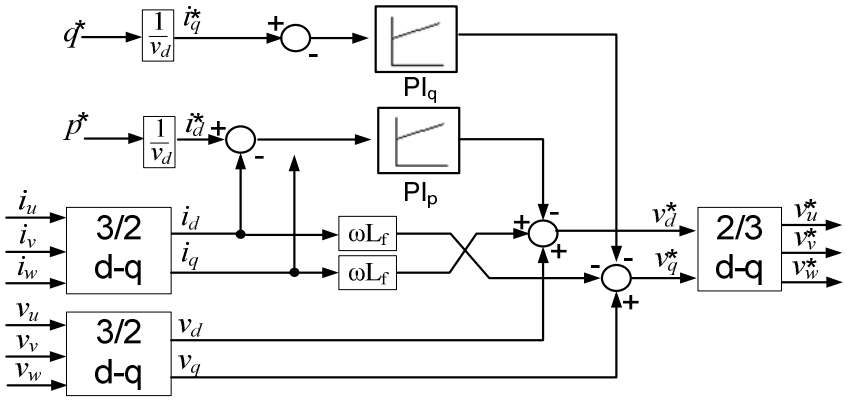


**Figure 27** *Main operative scheme of the decoupled current control method.*

The *d-q* transformation applied to L/filter leads to following equation ( 2 ).

$$\begin{cases} v_{Sd} - v_d = L_f \dfrac{di_d}{dt} - \omega L_f i_q \\ v_{Sq} - v_q = L_f \dfrac{di_q}{dt} + \omega L_f i_d \end{cases} . \qquad (2)$$

Where $v_d(i_d)$ and $v_q(i_q)$ are respectively the *d*-axis and the *q*-axis component of $v(i)$. In the same way $v_{sd}$ and $v_{sq}$ are the *d*- and *q*-axis component of $v_s$. The Active and reactive power can be expressed with the following equation ( 3 ):

$$\begin{aligned} p &= v_{Sd} \cdot i_d \\ q &= v_{Sd} \cdot i_q \end{aligned} \qquad (3)$$

The line space vector voltage, $v_s$, is oriented along the d-axis of the rotating stator frame. For this reason active and reactive power can be controlled independently by means of the proper control of $i_d$and $i_q$.

The active power reference value, $p^*$, is evaluated, taking into account the charging current required by the different sub-modules on each branch, by means of the following equation ( 4 ),.

$$p^* = \sum_{j=1}^{n} v_{c_{i,j}} \cdot i^*_{c_{i,j}} \qquad (4)$$

Where n is the number of SSM and the index $i=u,v,w$ is related to each branch. For the proper control of the reactive power, its reference value, $q^*$, is set to zero.

The presented control scheme, reported in Figure 27, aims to compensate the effect of source voltage and steady-state drop voltage across the filter inductance. In this scheme, two current PI controller give, as output, the $v_d^*$ and $v_q^*$ voltage reference signals. The three phase voltage reference values are obtained by means of the inverse *d-q* transformation.

*SoC Balancing Control*

Following the hierarchical control scheme reported in Figure 26 the SoC balancing control can be divided into SSM charge control and cluster balancing control [46]. The first control scheme, as reported inFigure 28, is related to the control of the State of Charge of each storage unit.

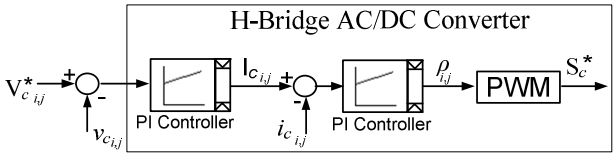


**Figure 28** *SSM Charge Control.*

In Particular, this scheme is based on the proper management of the first H-Bridge AC/DC converter, which controls the actual voltage, $v_{c_{i,j}}$, of each storage taking as reference the value, $V^*_{c_{i,j}}$,of its maximum charging voltage. On the base of the comparison between the above voltage values, a PI controller gives as output the reference current, $I^*_{c_{i,j}}$. Then, a second PI controller is devoted to the evaluation of the modulation index, $\rho_{i,j}$, of the converter in order to control the charging current for the related storage unit.

The cluster balancing control, reported in Figure 29, has the aim to keep the DC mean voltage of the controlled branch $V_{c_i}$ equals to the DC mean voltage among the three branches.

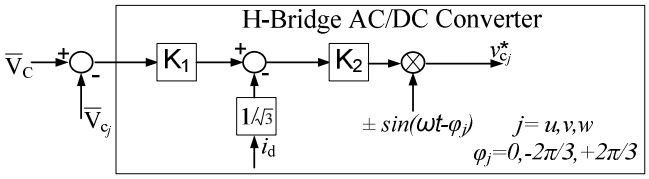


**Figure 29** *Clustered Balancing Control.*

In this case the DC mean voltage can be defined by the following equation ( 5 ):

$$\bar{V}_c = \frac{1}{3} \cdot \left(v_{c_u} + v_{c_v} + v_{c_w}\right) \qquad (5)$$

The clustered balancing control produces the i-phase balancing signal $v^*_{c,i}$ as:

$$v^*_{c,j} = k \cdot \left(h\, \Delta v_{c_j} - i_d\right) \cdot \sin\left(\omega t - \varphi_j\right) \qquad (6)$$

where $\Delta v_{c_j}$ and $i_d$ are both DC signals. The DC output signals of the minor current are converted into AC signals, on the *u,v,w* branches, respectively through their multiplication for the term sin(ωt), sin(ωt−2π/3) and sin(ωt + 2π/3).

The reference signals for each sub-module are given by the sum of three phase voltage active power components $v^*_u$, $v^*_v$ , $v^*_w$, coming from the decoupled current method, and three phase voltage of the clustered balancing control $v^*_{c,j}$ *j=u,v,w.*

*PEV Charge Control*

The charging operations of the connected PEVs are related to the proper control of the H-Bridge DC/DC isolated converter. The main operative scheme of this converter is reported in Figure 30

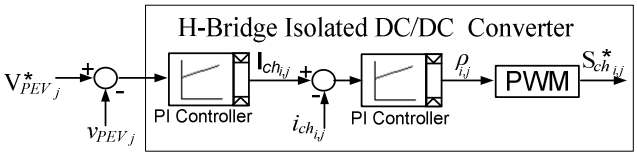


**Figure 30** *Main control scheme of the H-Bridge isolated DC/DC converter during the PEV charging operations.*

In this case, each $SSM_{ij}$ is controlled on the base of the comparison between the maximum charging voltage of the PEV battery pack, connected to $branch_j$, and its actual value. Then the control evaluates the required recharging current and the switching sequence for the PWM control of the converter.

## *Conclusions*

This chapter has been mainly focused on the analysis of charging infrastructures, which play an important role in supporting the wide adoption of PEVs. Starting from the different charging modes and connectors related to the SAE J1772 standard, AC and DC charging architecture has been considered showing the advantages of using stationary energy storage buffers, which can support the main grid during the fast charging operations of PEVs in a smart grid scenario. Moreover the description of buffered architecture based on multilevel converters have evidenced the possibility of further benefits, in terms of voltage balancing among the energy storage cells and power quality, which can be obtained with the use of distributed configurations.

# **Chapter 3.** Energy storage systems for PEVs

***Introduction***

The advantages related to the electric mobility, in terms of high conversion efficiency and low pollutant emissions, justify the strong interest of researchers and manufacturers through the development of high performance battery technologies. In fact low travel range, high charging times and low durability of the battery pack, in terms of life cycles, have delayed in the past years the diffusion of electric vehicles on the market [49]. From this point of view, recent researches and experimentations have allowed reaching energy and power density values, which satisfy in most of the cases urban mobility requirements [50]. These technology advancements have encouraged automotive manufacturers to increase their investments in the production of electric and plug-in hybrid vehicles, which has overcome the prototype phase and are now ready for large-scale production. In addition new high power density storage technologies, such as super-capacitors, are expected to give further contribution in improving PEV performance, when connected in hybrid configurations with high energy density storage systems [51] [52].

This Chapter starting from an analysis of the main performance parameters related to energy storage systems (ESSs) for PEV applications, presents an overview on the different storage technologies with particular focus on lithium batteries and super-capacitors. Finally this Chapter describes the experimental setup for the laboratory characterization of energy storage systems with the main characteristics of the energy storage modules, which have been used for the experimental tests reported in Chapter 5.

### *3.1 Main performance parameters of energy storage systems*

Nowadays a large number of energy storage technologies, based on different chemistries, have been investigated in the literature and by automotive manufacturers [53][54][55]. In order to assess the performance of the different storage technologies, when supplying PEVs in their typical operative conditions, an identification of the main parameters related to the electrical behavior of the ESSs is required.

One of the most important parameters for ESSs is the *Capacity*. This value is generally measured in *Ah* and can be defined as the amount of charge, which is possible to drawn from a fully charged storage unit, until it reaches its minimum voltage value. It is important to notice that this value is generally referred in the literature to the actual capacity of the battery when it is discharged in exactly one hour. As a consequence if a battery is characterized by a capacity of 50 *Ah*, it will be fully discharged in one hour with a constant discharging current of 50 *A*. Nevertheless battery manufacturers use to refer the rated capacity to a specific discharging time, which is generally 5 *h* or 20 *h*, and report in form of table or graph the behavior of the capacity for different discharging current values. However the values of capacity reported in the datasheet can be considered reliable only for new batteries at a fixed constant temperature. In addiction the actual capacity value of a battery is generally strongly reduced for high discharging currents. This changing in the expected capacity is caused by the energy losses due to uncompleted or unwanted chemical reactions inside the cells [56]. The laboratory evaluation of the actual capacity of storage systems in different operative conditions is of great interest since it can give a first idea on the expected vehicle autonomy, when supplied by the ESS under test. New technologies of lithium batteries and super-capacitors are less affected by capacity losses with respect to lead acid batteries [57].

The *charging/discharging rate* of ESSs is defined as the maximum current, which can be used for storage systems charging/discharging operations without affecting their durability in terms of life cycles. This parameter is experimentally evaluated by the manufacturer and is reported in the datasheet as the ratio between the maximum allowed current and the rated capacity value. As a consequence the charging discharging rate should be reported in $h^{-1}$ ($h^{-1} = A/Ah$) but it is common use to represent this parameter followed only by the letter C, without any

measuring unit (*For this reason it is also called C-rate*). In particular a 50 *Ah* battery is discharged with a *C*-rate of 1 *C* when it is discharged with a current value of 50 *A*. New lithium battery technologies are able to easily reach 10 *C* discharging rate and about 3 *C* charging rate. This parameter is particularly relevant since it can define the maximum electric power supplied by the ESSs, during the peak power demand of the vehicle running on the road, and the maximum power supplied to the vehicle ESS during the charging operations.

The *State of Charge* (SoC) is the amount of residual charge available from an ESS evaluated as a percentage of its capacity. As a consequence the SoC, at the time $t_i$, can be calculated with the following equation ( 7 ):

$$SoC(t_i) = SoC(t_0) - \frac{\int_{t_0}^{t_i} i(t)dt}{C} \qquad (7)$$

Where $t_0$ represents the starting time of ESS charge/discharge operation and C is the ESS rated capacity. The SoC evaluation is generally taken into account for the assessment of the residual vehicle travel range. It is clear that the equation ( 7 ) can be considered reliable in the hypothesis that the value of $SoC(t_0)$ is well known and the battery capacity does not depend on charging/discharging current values. Actually the proper evaluation of SoC is generally affected by environmental temperature, ESS *State of Health* (SoH) and charging/discharging current values. For this reason the right evaluation of SoC, for different storage technologies, is still considered a topic worthy of literature investigation [58][59].

The *Energy Density* of an ESS can be defined as the electric energy stored per unit volume (*Wh/l*) or per unit weight (*Wh/kg*). The evaluation of the energy stored is generally referred to the rated value of voltage and capacity and can be calculated with the equation ( 8 ).

$$E(Wh) = V(V) \cdot C(Ah) \qquad (8)$$

The volumetric energy density (*Wh/l*) was introduced in the past since many batteries was characterized by liquid electrolytes. However, although the application of this kind of batteries is not considered in the automotive field, the unit volume is still considered useful since it can give a first idea on the dimensions of an ESS, which are required to respect the on board space constraints of PEVs. The gravimetric energy density (*Wh/kg*) is usually referred as specific energy and can be considered in order to evaluate the weight of an ESS, which have to respect the on board weight constraints of PEVs. On board weight limits are generally

more restrictive than space constraints, for this reason the scientific and technical literature generally refer to the specific energy.

The *power density* can be defined as the power obtainable by an ESS per unit volume (*W/l*) or per unit weight (*W/kg*). In the latter case this parameter is generally referred as specific power. The evaluation of specific power needs to take into account that it is not convenient to operate the battery at its maximum power for a long time since the battery life might be seriously compromised.

The *energy storage durability* is defined by the number of charging/discharging cycles that an ESS can perform, without reducing its actual capacity. Generally, for this evaluation, the actual capacity is considered acceptable until it reaches the value of 80% of the ESS rated capacity [26]. The ESS durability is strongly affected by the working temperature and by ESS Depth of Discharge (DoD), which is given by the following formula for the related time of evaluation $t_i$:

$$DoD(t_i) = 100\% - SoC\ (t_i) \qquad (9)$$

For this reason ESS manufacturers strongly recommend to not overcome the DoD value of 20 % during the ESS discharging operations. It is clear that a high ESS durability would be required for PEV applications since it strongly affects the maintenance costs [60][61].

The *Amperhour Efficiency* of an ESS, also referred as *Columbic Efficiency*, is defined as the ratio between the amperhours supplied, during ESS charging operation, and the amperhour that is possible to drawn from the ESS, during its discharging operation. In the same way the *Energy Efficiency* can be defined taking into account also ESS voltage values. Columbic and energy efficiencies are generally affected by current values involved both in the charging and in the discharging operations. For this reason the efficiency evaluations are generally referred to specific charging and discharging procedure.

Following the above definitions, it is clear that an ESS suitable for automotive applications is expected to satisfy different requirements, which can be summarized as follows [62]:

- High specific energy. This requirement involves the extension of all electric range for the vehicle, reducing at the same time the number of charging/discharging cycle of the battery pack.

- High specific power. The use of high specific power ESS enable the possibility to increase the acceleration performance of PEV, reducing at the same time the vehicle charging time without losses of ESS durability.
- High durability. As already mentioned above, this parameter can reduce the maintenance cost of the on board ESS, which is one of the critical issues for the diffusion of PEV on the automotive market.

Finally, also environmental aspects, which are mainly related to the use of toxic materials, need to be properly taken into account in the choice of the ESS.

Different storage technologies are now available on the market and can be used for different purposes. Among those, electrochemical batteries and super-capacitors are considered the most promising technologies for their application in the automotive field.

### *3.2 Electrochemical batteries*

#### *3.2.1 Lead Acid Batteries*

Lead-acid batteries have been largely used in the past for industrial and electric traction systems. The elementary cell of a lead storage unit is characterized by a negative electrode of metallic lead and a positive electrode of lead dioxide, whereas the electrolyte is realized by means of an aqueous solution of sulfuric acid with high ionic conductivity [63]. Different technologies have been investigated during the years and can be classified in two main categories: flooded and valve regulated (VRLA) lead acid batteries. The latter mentioned technology was developed in order to solve the issues of flooded batteries mainly related to the drying of the cells, which requires the frequent control of the distilled water level inside the battery. For this reason VRLA are also called no maintenance batteries since they need minimal attention and maintenance operations by the user.

Lead acid batteries are characterized by a voltage per cell of about 2.0 *V*, an energy density in the range 35÷50 *Wh/kg* and a specific power of 150 *W/kg*. As a matter of fact, in comparison with new lithium technologies, this kind of storage system presents disadvantages in terms of very low energy density, low performance at high discharging currents, low charging rate and high environmental impact. These disadvantages have strongly affected the use of lead-acid battery for supplying road electric vehicles. However this battery technology

still finds a large acceptance in other kinds of applications, especially in the industrial sector and for stationary storage, where restrictive constraints in terms of volume, weight and charging rate are not required. Their widespread utilization is justified by the fact that lead acid batteries are particularly secure, with respect to other technologies. In addition their cost is considerably cheap and their operative conditions are less affected by environmental temperature, with respect to other storage technologies. In conclusion lead acid batteries represent a well-known battery technology and for this reason their behavior is often used also as reference in order to evaluate the performance of other storage technologies [64] [57].

### *3.2.2 Lithium Batteries*

Nowadays, new energy storage technologies based on lithium compounds are catching great attention in the automotive field. This is mainly due to their characteristics of high specific energy and specific power, which allow supplying PEV with high performance in terms of acceleration and driving range.

In fact, lithium has been recently considered as an attractive metal, to be used as anode material, since it is characterized by lightness and high potential. Nevertheless its utilization in the automotive sector involves different issues related to safety hazard, which are mainly due to the high reactivity of this metal. As a consequence, in lithium-ion batteries, both positive and negative electrode are realized by using "lithium host" compounds, where an intercalation process occurs. In this case lithium ions can be reversibly removed or inserted without any significant structural change in the host. The negative electrode is generally based on graphitic carbon, whereas the positive electrode is realized using a metal oxide based on lithium compound, which can be in the form Li"M"$O_2$ or Li"M"$O_4$. In this case the letter "M" indicates a metal, which is generally represented by Cobalt (Co), Nickel (Ni) or Manganese (Mn). The resultant electrochemical reaction involves a cyclic transfer of lithium ions from the cathode (the lithium source) to the graphite anode, with no presence of metallic lithium. The cell voltage is 3.8 V at 25 ° C. This type of battery has been proposed for vehicle applications with solid electrolytes constituted by polymeric materials, able to transfer lithium ions between electrodes [50]. In this case, the absence of liquid phases simplifies the realization of leak-proof and light-weight containers, which represents an additional advantage for on board ESSs. In particular, it is possible to realize

sandwich of foils, characterized by packaging flexibility and insensitivity to shock/vibration damage, as required by many car manufacturers.

Recent developments in the field of lithium batteries have been focused on the possibility to reach very high energy and power densities by using new types of anode and cathode. In particular, the researches about the cathode of lithium ion batteries have been intensively oriented on high voltage spinels and high capacity layered lithium metal oxides. The $LiCoO_2$, or Li-Co-Mn mixed oxides are commonly used in lithium ion batteries as cathode materials. These compounds are characterized by interesting performance in terms of high capacity, good rate capability and skill to operate at high voltage. The main limitation of this type of cathode material is constituted by the cost of cobalt and battery stability, which could not be considered optimal during the recharging phases [4].

It is important to observe that lithium battery pack are generally realized with different cells, which are generally connected in series. The cells realizing the battery pack, at the beginning of its life, are completely balanced and present the same cell voltage value. Unfortunately, during the charging and discharging operations of the battery pack, the voltage value of each cell can change, with a slight difference in comparison with the other cells, on the base of its temperature, SoH and internal resistance. This phenomenon is generally cause of voltage unbalance, which represents a condition to avoid in order to keep the battery safe and preserve battery durability. In fact during charging and discharging operations, in case of voltage unbalance among the cells, over-charge or under-charge conditions may happen since only the whole battery pack voltage is measured. In order to avoid these conditions, lithium batteries are generally equipped with a Battery Management System (BMS). A BMS is an electronic device which controls the voltage balance among the cells and interrupts the circuits at the battery terminals in case of under/over-voltage conditions, short circuit and overheating conditions [65].

As an example, a picture of a 20 $Ah$ – 49 $V$ $Li[NiCoMn]O_2$ battery pack with its BMS is reported in Figure 31.

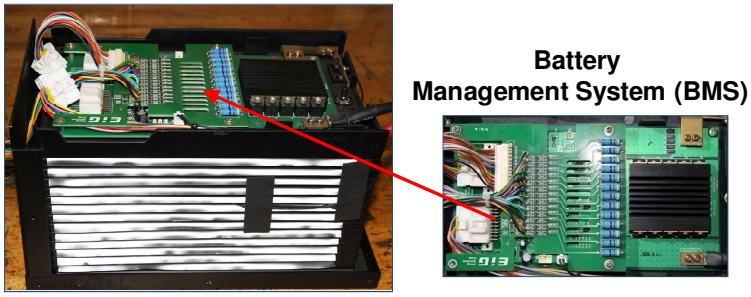


**Figure 31** *Picture of Li[NiCoMn]$O_2$ Battery Pack with its BMS.*

Recently, other low-cost cathode materials have been studied and proposed with the main aim of reducing cost and increasing both safety and reliability of lithium based batteries. In particular $LiFePO_4$, based on olivine crystal structure, have shown promising characteristics for their application to supply road electric and hybrid vehicles [66][5] [67]. The main advantages of $LiFePO_4$ batteries are based on the low cost and high availability of the metal iron together with high thermal stability and safety properties, mainly related to the strength of the covalent Fe-P-O bond, which reduces the risk of oxygen release [68]. Their energy density is lower than $LiCoO_2$ cathode technologies, but their main limitation is represented by the high values of internal resistance, which is cause of losses and affects battery efficiency [68]. As example, a picture of a 300 *V* - 60 *Ah* $LiFePO_4$ battery pack is reported in Figure 32.

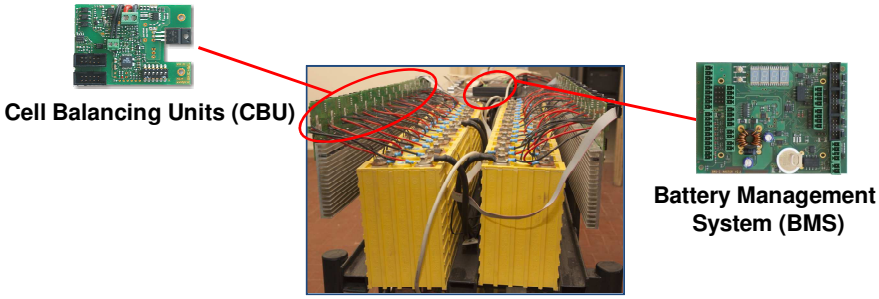


**Figure 32** *Picture of $LiFePO_4$ battery pack with BMS and CBU.*

In the above picture also the Cell Balancing Units (CBU), which allow BMS to monitor and control each cell, are reported.

The above mentioned lithium technologies are characterized by an energy density up to 200 *Wh/kg*, which results in an all-electric travel range of about 150 *km* for a PEV supplied by these battery packs. The new challenge for the researchers is the increasing in durability and charging rates of lithium battery

technologies in order to reduce more and more the vehicle charging times. In this context an interesting recent technology is represented by lithium–titanate battery ($Li_4Ti_5O_{12}$, also known as LTO), which is a modified lithium-ion battery that uses lithium-titanate nanocrystals on the surface of its anode instead of carbon graphite [69][70]. Although LTO storage units are characterized by rated voltage per cell of 2.4 *V*, which is lower than $LiCoO_2$ and LFP, they present great advantages in terms of durability, safety and charging rates. In fact these batteries can support charging rates higher than 10 *C*, which means that they can perform a complete recharge in less than ten minutes. The LTO based batteries have also the characteristic of an operating temperature range wider than other lithium battery technologies, in particular they have excellent low-temperature discharge characteristics with an actual capacity of 80% at 243 *K*. Moreover, their life span and power density are not lower than other lithium batteries, and their charging efficiency can be even higher than 98%. On the other hand, the energy density of 65 *Wh/kg* for the LTO batteries is higher than lead acid technology, but it is still lower than the other lithium based batteries [71].

### *3.3 Capacitors*

In order to improve PEV performance during acceleration and regenerative braking operations, ESSs are required to support high values of discharging/charging electric power. The existing battery technology is mainly devoted to increase energy density and is generally characterized by a durability, which is strongly affected by high values of charging/discharging current. For this reason high specific power storage devices, such as capacitors are becoming an interesting solution to power electric vehicles, in combination with battery packs, realizing hybrid energy storage systems. Among capacitor technologies, electrochemical double layer, also referred as super-capacitors, and Lithium-ion Capacitors represent the two most attractive solutions for automotive applications,

#### *3.3.1 Electrochemical double layer capacitors*

Electrochemical double layer capacitors (EDLCs) combine high power density and durability, in terms of life cycles, with higher energy density values, compared with traditional capacitors technologies, such as electrostatic and electrolytic capacitors.

EDLCs are almost similar in construction to traditional electrostatic capacitors. The main differences are related to the presence of a conductive electrolyte salt in direct contact with the metal electrodes, whereas a separator provides insulation between the electrodes and allows the transfer of ions [72]. In addition EDLCs electrodes are characterized by a porous structure, which allows reaching greater capacitance per unit volume, with respect to the traditional capacitor technologies. In fact the capacitance ($C=\varepsilon_0 A/d$) can be increased thanks to the possibility of reducing the separation $d$ between the electrode surface and the ionic charges. A simplified scheme of an EDLC is reported in Figure 33 [73].

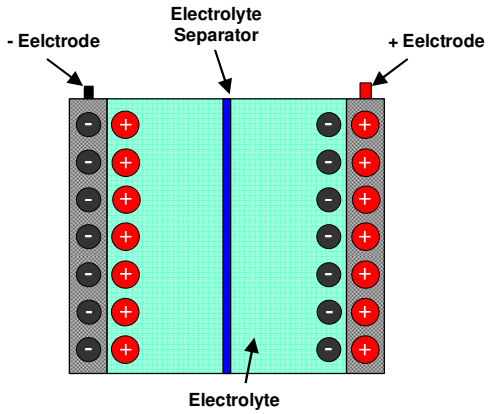


**Figure 33** *Simplified scheme of an EDLC.*

The higher energy density, with respect to traditional capacitor technologies, is due to the porous structures of the EDLCs electrode surface, realizing equivalent areas up to 2000 $m^2/cm^3$. The rated cell voltage for an EDLC is of about 2.6 V [74].

Different materials, such as carbon materials, mixed metal oxides and conducting polymers, have been proposed in literature to be used for super-capacitor electrodes [72]. In particular, interesting performance has been obtained with carbon technology in its various forms such as carbon cloth, activated carbons and carbon nano-tube [75]. In recent years, graphene has also been considered as a promising capacitor electrode material. This is mainly due to the characteristics of chemical stability, high electrical conductivity and large surface area of this material [76].

### *3.3.2 Lithium-ion capacitors*

The need for a rechargeable energy storage device that provides both high energy and high power densities justifies the growing attention of the research towards new lithium based capacitor technologies.

In this context lithium-ion capacitors (LiC) has been proposed as a mixed solution between lithium-ion batteries and EDLCs. This capacitor technology is based on the use of two different materials for positive and negative electrodes and, for this reason it can be classified as an asymmetric or hybrid storage technology. In particular, as reported in Figure 34, lithium-ion capacitors are realized with a traditional lithium battery electrode, characterized by Li intercalated hard carbon anode, and a double-layer cathode electrode [77].

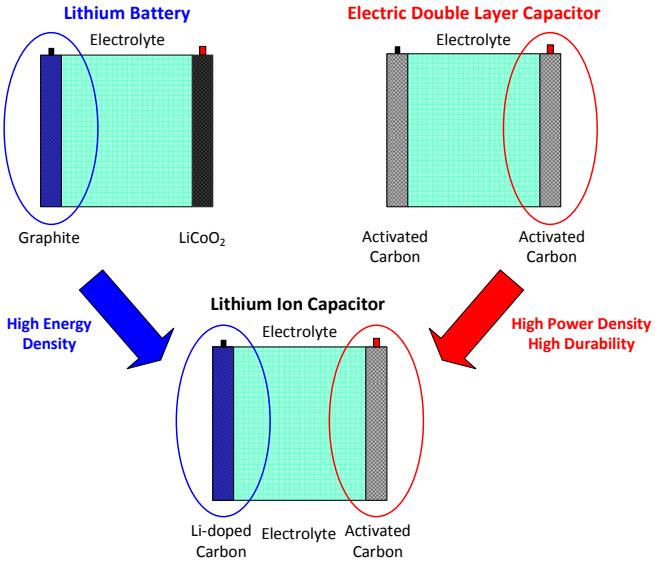


**Figure 34** *Simplified Scheme of lithium-ion capacitors.*

During charge and discharge operations, the behavior of each electrode realizing the LiC cell is similar to their behavior in the respective non-hybrid devices (Lithium-ion battery or EDLC) [78]. For this reason the potential of the anode remains low while the potential of the cathode rises and falls during the different charging/discharging operations. In this regard Figure 35 reports a comparison among the behavior of the electrode voltage for the case of EDLC (A) and LiC (B).

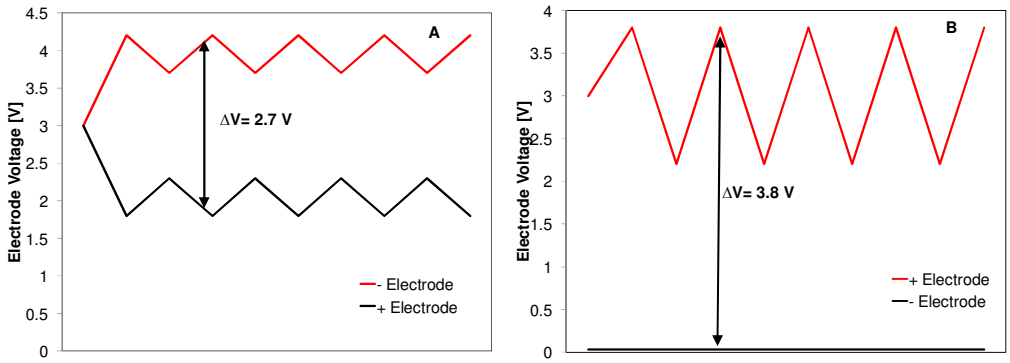


**Figure 35** *Electrode voltage behavior during charging and discharging operations for EDLCs (A) and LiC (B).*

The above comparison clearly justifies the higher energy density of LiCs, due to their higher nominal voltage. In fact, in the case of EDLCs, the voltage of the cathode and anode vary symmetrically as activated carbon is used for both electrodes and lower values of nominal voltage can be obtained.

In order to summarize the storage technologies analyzed in this chapter, Figure 36 reports a comparison among these technologies in terms of Energy Density vs Power Density.

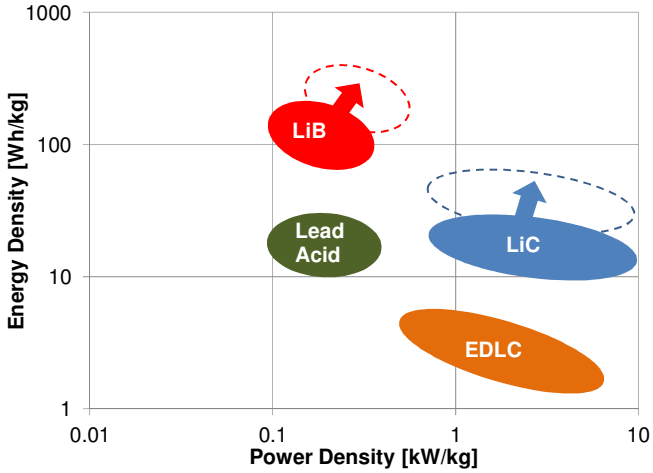


**Figure 36** *Comparison among different storage technologies.*

As it can be clearly observed from the above comparison, new lithium battery and capacitor technologies pursue the same objective of reaching high values of energy density combined with high values of power density.

### *3.4 Laboratory test benches for experimental analysis on energy storage systems*

As mentioned in the above paragraphs the performance of energy storage systems are strongly affected by their real operative conditions. For this reason different papers have focused the attention on the experimental analysis of the above technologies, in order to support the lack of knowledge on the actual behavior of storage systems [26] [57] [78] [79].

During the research activities reported in this manuscript, an experimental analysis on battery modules of different technologies has been realized through a laboratory test bench, whose block scheme is reported in Figure 37[57] [79].

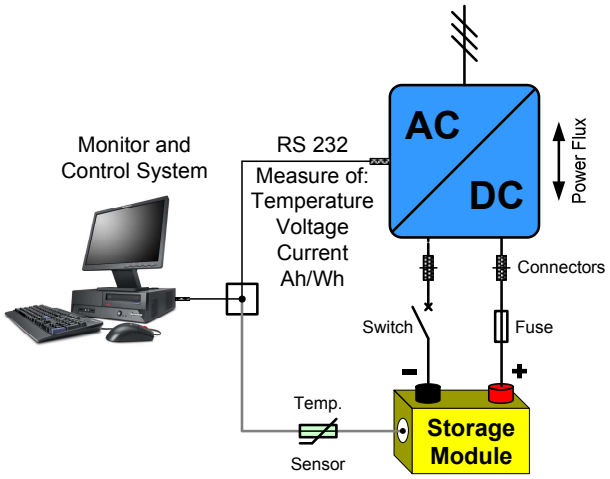


**Figure 37** *Laboratory test bench for battery characterization.*

The main architecture of the above test bench, also referred as *Life Cycle Tester*, is based on bidirectional AC/DC power converter, which is controlled by means of a specific software interface based on RS232 communication protocol. The software interface allows the main electrical parameters, such as battery voltage, current, power and temperature to be set as reference, monitored and acquired. In this way the battery packs under study can be characterized through charging and discharging tests at constant current/voltage/power values. In addition the above electric parameters can be set, in order to follow different profiles, as sequences of phases, with a transition time between two consecutive phases of about 900 *ms*. Thanks to the above control modes allowed by the laboratory test bench, the real working conditions of the single battery module supplying an

electric traction drive can be simulated and analyzed. The main electric characteristics of the life cycle tester are reported in Table 2.

| | |
|---|---|
| AC Input [*V*] | 400 AC |
| Max Output Voltage [*V*] | 18 DC |
| Max Output Current [*A*] | 100 |
| Output ripple | 7 % Irms at full range |
| Transition time From CH to DISCH | 900 ms |
| Efficiency | 0.91 |
| Power Factor | 0,78 |
| Cooling | Forced Air |
| Protection degree | IP 21 |

**Table 2** *Main characteristics of the Life Cycle Tester.*

As it can be observed from the above table, the thyristor pulse technology and appropriate choke allow to reduce the ripple current down to 7% rms, to obtain fast transient response times and a good accuracy to follow the references.

The above laboratory test bench has been used in order to carry out experimental analysis on the charging efficiency of different battery packs, which is reported in Chapter 5. Dynamic tests have also been carried analyzing the behavior of these battery technologies, when supplying an electric drive coupled with an eddy current brake for the simulation of standard driving cycles [57].

The energy storage modules, which have been considered for the above tests, are based on $LiFePO_4$ and $Li[NiCoMn]O_2$ chemistries whereas a lead acid module has been considered as reference. The main characteristics of these battery modules are reported in Table 3.

| | **Lead acid** | **$Li[NiCoMn]O_2$** | **$LiFePO_4$** |
|---|---|---|---|
| Nominal Battery Voltage [*V*] | 12.0 | 14.6 | 12.8 |
| Nominal Capacity [*Ah*] | 40 | 40 | 40 |
| Nominal Energy [*Wh*] | 480 | 584 | 512 |
| Specific Energy [*Wh/kg*] | 25 | 176 | 80 |
| Energy Density [*Wh/l*] | 67 | 350 | 142 |
| Maximal continuous discharge current [*A*] | 200 (5 *C*) | 200 (5 *C*) | 120 (3 *C*) |
| Peak discharge current [*A*] | 800 (20 *C*) | 400 (10 *C*) | 800 (20 *C*) |
| Specific Power [*W/kg*] | 660 | 1700 | 1600 |
| Durability (Cycle Life at 80% DOD) | 500 | 1000 | 3000 |

**Table 3** *Main characteristics of Lead acid and Li battery modules.*

***Conclusions***

In this chapter the main electric parameters of energy storage systems have been identified in order to evaluate their performance, when supplying road electric and plug-in hybrid vehicles. In addition a detailed analysis of traditional and innovative chemistries, related to battery and capacitors, is reported with a comparison among different storage technologies in terms of energy density and power density. This analysis have shown the main advantage of using hybrid storage systems which combine the high energy density, related to lithium batteries, with high power density and durability related to super-capacitors. Finally the test bench, which is used for the laboratory characterization of energy storage systems, has been presented with a description of the main characteristics and control modes. The obtained experimental results of these laboratory tests are reported in Chapter 5 for different storage technologies.

# **Chapter 4.** Case Study: Laboratory prototype of a DC fast charging architecture

***Introduction***

Nowadays, different solutions have been proposed in the literature in order to realize fast charging architecture based on the use of AC or DC bus. In this regard many papers have focused their attention on the identification of energy management strategies for charging stations with renewable energy sources and stationary energy storage systems. Nevertheless, these papers are mainly based on simulation activities, without focusing the attention on experimental analysis and validations [7] [80] [81]. These kinds of activity can find further supports in experimental evaluation, based on a laboratory prototype, mainly aimed to compensate this lack of information with real data.

This Chapter reports a description of a laboratory prototype of DC fast charging architecture, which is considered as case study for the experimental evaluations of this work. This prototype has been designed and realized during the research activities described in this manuscript. The main criteria adopted for the designing of the prototype are reported at the beginning of this chapter with some details on the simplified model used for preliminary theoretical analysis. Then a description of the main characteristics of DC/DC and AC/DC power converters, realizing the laboratory prototype, is reported with particular focus on their specific topologies. Moreover the main power fluxes and energy management strategies, which allow the experimental characterization of the prototype in its different operative conditions, are described with detailed information on the control scheme of each power converter.

### *4.1 Design criteria of DC fast charging architecture*

Starting from the considerations, reported at the end of Chapter 2, about the real advantage of using DC charging architecture based on stationary energy storage buffer, a prototype of buffered architecture has been designed and realized on the base of the power scheme reported in Figure 19 of Chapter 2, in order to perform laboratory tests in different operative conditions.

The design procedure of the prototype has been supported by a simulation activity whose main results are reported in [82]. In particular a simplified model of the DC fast charging architecture has been realized in Matlab-Simulink environment. This activity has been realized taking advantage of the Sim-Power systems tool, which is a powerful library specifically devoted to the simulation of electric components. The main scheme of the evaluated model, for the DC-Link side, is reported in Figure 38.

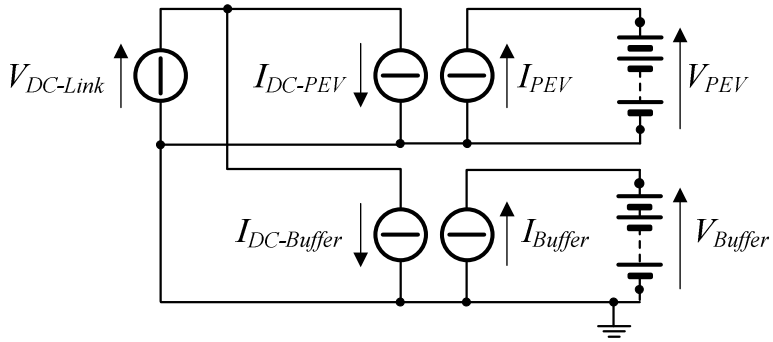


***Figure 38*** *Block Scheme of the Simulink model for DC-Link side of the DC fast charging architecture.*

The modelling procedure of the proposed architecture is mainly focused on the evaluation of the main power fluxes within the charging station and on their control, which aims to optimize charging times and impact on the main grid in terms of power requirements during vehicle fast charging operations. This preliminary simulation study has been carried out without taking into account the PWM modulation and energy losses of the power components, since these evaluations are not considered useful to determine and evaluate the different energy management strategies. In this hypothesis the AC/DC power converter has been simulated represented through an ideal Voltage Controlled Voltage Source (VCVS) representing the DC bus with a constant voltage value. This value has been set at 790 V, considering the AC/DC power converter realized as a voltage

source active rectifier, characterized by an input voltage of 400 *V* AC. Moreover, in a similar way, the behaviour of both the two DC/DC converters considered is simulated Current Controlled Current Sources (CCCS), which are controlled by means of the following equations ( 10 ) to obtain the charging/discharging operations of the related battery packs.

$$\begin{cases} V_{DC-Link} I_{DC-Buffer} = I_{Buffer} V_{Buffer} \\ V_{DC-Link} I_{DC-PEV} = I_{PEV} V_{PEV} \end{cases} \quad (10)$$

In particular equations ( 10 ) have been evaluated without taking into account the efficiency losses of each converter.

On the base of the evaluations obtained through the above described simulation activity the laboratory prototype has been realized in collaboration with the MsC Oy, which is a Finnish company operating in the field of power electronics. The DC bus conversion stage is obtained by means of an AC/DC bidirectional power converter, which is connected to the three-phase low voltage AC network, through a 20 kVA insulation power transformer. In this case, the possibility of the grid-tied converter to manage bidirectional power fluxes also allows the realized DC micro-grid to perform V2G operations. The use of insulation power transformer is justified by the fact that galvanic insulation is not provided by the converters realizing the DC micro-grid. The integration of buffer and PEV battery pack with the DC-Link is featured by means of two DC/DC power converters. In particular, the DC/DC converter related to the energy storage buffer is required to manage bidirectional power fluxes in order to perform charging, discharging and islanding operations. In addition, both the DC/DC converters are designed to to interface their output with a large variety of battery packs, characterized by different values of charging voltage and charging/discharging rates. However the rated voltage values, which has been taken as reference in order to carry out the experimental tests reported in the following Chapter, have been selected as 50 *V* for the vehicle on charge and 288 *V* for the energy storage buffer. In the first case, the voltage value of 50 *V* is typical for full electric two wheelers, whereas the value of 288 *V*, chosen for the energy storage buffer, is typical for full electric cars and allows also analysing V2G operations. The information exchange and communication protocols among PEV, buffer and the charging architecture is not analysed, since it is not considered the main aim of this work.

### *4.2 Characteristics of power converters realizing the laboratory prototype*

The electric scheme of the AC/DC grid tied converter is reported in Figure 39 [67].

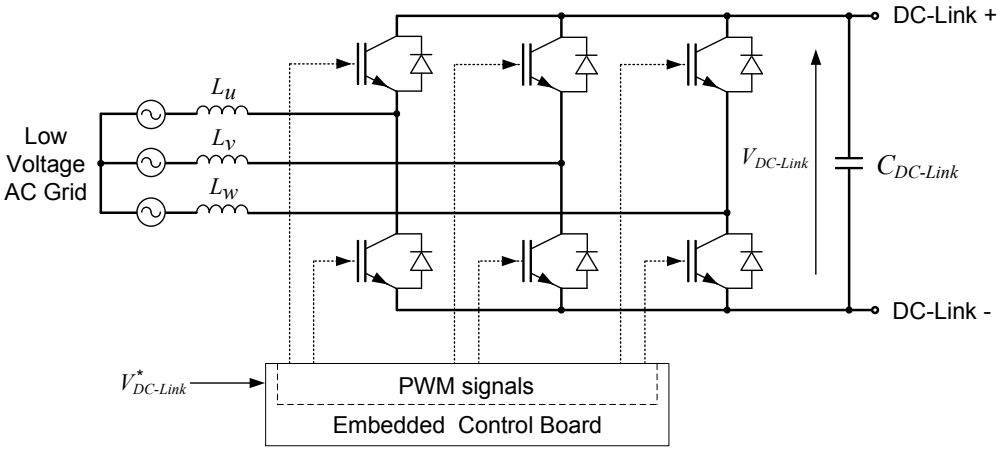


**Figure 39** *Electric scheme of the AC/DC converter.*

In particular, the selected grid-tied converter is a full bridge three-phase active front-end converter, based on 1200 *V* Semikron IGBT devices with a DC-Link voltage reference set at 790 *V*. The choice of this high reference voltage value allows interfacing the charging architecture also with high voltage energy storage systems. In addition this choice is required in order to reduce the current involved on the DC-bus during the different operative conditions, with positive consequences on the sizing of electric protections and conductors.

The main operative parameters of the bidirectional AC/DC grid-tied converter are reported in Table 4.

| **Model** | MSC 32DCAC750ME |
|---|---|
| **Power Fluxes** | Bidirectional |
| **DC-Link Side** | |
| DC Voltage [*V*] | 790 |
| Rated Current [*A*] | 32 |
| **AC Three-Phase Side** | |
| Main Grid Voltage [*V*] | 380-480 @ 50/60 Hz |
| Rated Current [*A*] | 32 |
| Rated Power [*kVA*] | 20 |
| **Control Mode** | DC Link Voltage Reference |
| **Rated Efficiency [p.u.]** | 0.96 |

**Table 4** *Main characteristics and operative conditions of the AC/DC grid-tied converter.*

It is clear that, although the DC rated current of the grid tied converter is 32 *A*, the DC bus is designed to support current values up to 200 *A* in order to enable the energy sharing among existing and future storage/generation units on the DC bus.

The selected DC/DC bidirectional converter is devoted to the management of the power fluxes related to the considered energy storage buffer. The electric scheme of this converter is reported in Figure 40 [67].

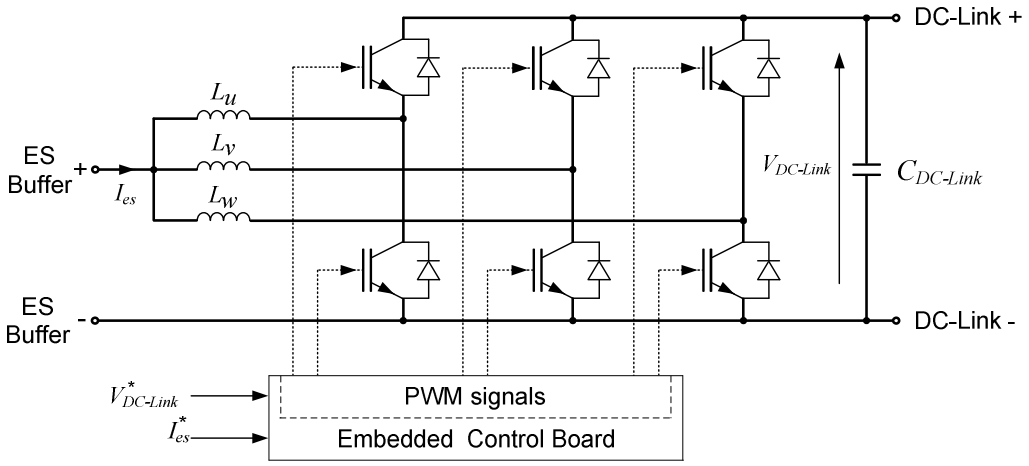


**Figure 40** *Electric scheme of the bidirectional DC/DC converter.*

In particular the topology of this converter is based on interleaved full-bridge architecture. In this case the converter legs are electrically connected in parallel trough three identical 2 *mH*/30 *A* inductances. The considered interleaved architecture for this power converter presents different advantages in terms of reduction of current ripple in comparison with single-phase topologies of the same rated power [83]. The 20 *kHz* pulse-width modulation (PWM) control of this converter is devoted to perform energy storage current reference and DC-Link voltage reference control modes trough the proper switching sequences of the six IGBTs. In addition also the current balancing among the three legs of this interleaved power converter is performed trough the PWM control. The embedded control board allows user to set the energy storage current and the DC-Link voltage reference by means of analogue voltage signals. In the first case the direction of power flux can be control trough a specific digital input signal. In this way the converter can be controlled both as a current source converter, using the energy storage charging/discharging current, $I^*_{ES}$, as reference, and as a voltage source converter, using the DC-Link Voltage, $V^*_{DC\text{-}Link}$, as reference. Table 5 summarizes

the main characteristics and operative conditions of the bidirectional DC/DC converter.

| **Model** | MSC 60DCDC750DE |
|---|---|
| **Power Fluxes** | Bidirectional |
| **DC Link Side** | |
| Voltage range [*V*] | 100 - 800, DC |
| Rated Current [*A*] | 20 |
| **ES Side** | |
| Voltage [*V*] | 100-750, DC |
| Rated Current [*A*] | 20 |
| **Control Mode** | - ES Current Reference<br>- DC-Link Voltage Reference |
| **Rated Efficiency [p.u.]** | 0.96 |
| **Input Signals** | Digital Signal: Charge/Discharge, Control mode selector (V/I)<br>Analog Signals: $I^*_{Buff}$ = Current Reference on the ES side (0-10 *V* = 0-20 *A*); $V^*_{DC\text{-}Link}$ = DC-Link Voltage Reference (0-10 *V* = 0-710 *V*) |
| **Output Signals** | Analog Signals: $I_{Buff}$ = Energy Storage Current and/or $V_{DC\text{-}Link}$ = DC-Link Voltage (0-10 V) |

***Table 5*** *Main characteristics and operative conditions of the bidirectional DC/DC power converter.*

Differently from the above case, the topology of the DC/DC converter related to the vehicle battery pack is based on a simple unidirectional buck architecture driven by 11 *kHz* PWM technique. This choice is justified by the main function of this converter, which is limited to the charging operations of the two-wheelers battery packs. These battery packs are generally characterized by low performance in terms of rated capacity and voltage, since they are not required to support heavy vehicles for long travel distances. For this reason the possibility of realizing V2G operations, with the 790 V DC-Link supplied by the vehicle battery pack, is not considered a requirement for this converter. The main operative parameters of the DC/DC unidirectional power converter are similar to those of bidirectional converter, with the only difference that in this case the DC link voltage reference control mode is missing.

A Picture of the power converters integrated in the demonstrator and the complete laboratory setup are reported in Figure 41.

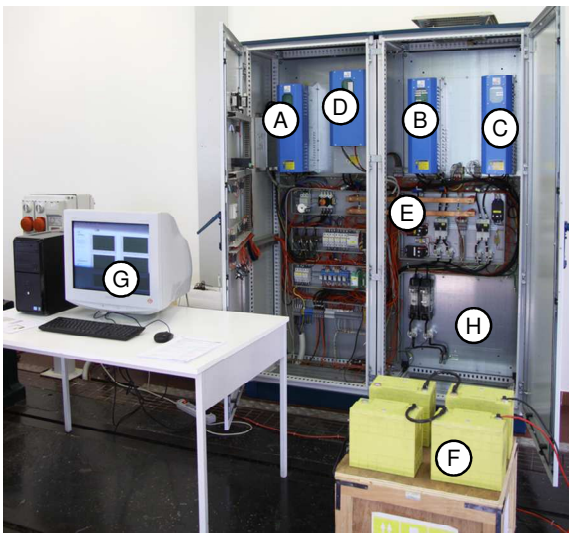


A – AC/DC Bidirectional Converter

B– DC/DC Bidirectional Converter

C – DC/DC Unidirectional Converter

D – DC/DC Bidirectional Converter for future RESs/ESs Integration

E – DC-Link

F – PEV Battery Pack On Charge

G – Monitoring PC

H – Additional Space for Future Extension

**Figure 41** *Picture of the charging station demonstrator.*

The 790 *V* DC-Link is realized by means of the copper bars (E), which are visible in the middle of this picture. Other components are also included in the rack order to support the measurement/control system and to guarantee the electric safety. An additional converter (D) is included in order to perform future integration of renewable energy sources.

The experimental tests on the prototype, reported in the following Chapter, are carried out using two different battery packs, characterized by different chemical composition and rated voltage. The main characteristics and operative working conditions for these battery packs are reported in Table 6.

| | **Lead acid** | **$LiFePO_4$** |
|---|---|---|
| Nominal Battery Pack Voltage [*V*] | 288 | 51.2 |
| Nominal Cell Voltage [*V*] | 2.0 | 3.2 |
| Number of Cells | 6x24 | 4x4 |
| Nominal Capacity $C_{10}$ [*Ah*] | 40 | 40 |
| Nominal Energy [*kWh*] | 11.5 | 2.0 |
| Specific Energy [*Wh/kg*] | 25 | 80 |
| Energy Density [*Wh/l*] | 67 | 142 |
| Maximum Ch. Voltage [*V*] | 334 | 64 |
| Minimum Disch. Voltage [*V*] | 230 | 41.6 |
| Maximum Ch. Current [*A*] | 8 (0.2 C) | 120 (3 C) |
| Maximum Disch.Current [*A*] | 200 (5 C) | 120 (3 C) |
| Max Peak Disch. Current [*A*] | 800 (20 C) | 400 (10 C) |

**Table 6** *Main characteristics of the Lead acid and $LiFePO_4$ battery pack used for the laboratory tests with the prototype.*

In particular, for the above tests, the 51 $V$ – 40 $Ah$ LiFePO4 battery pack, provided by Winston Battery is considered as representative of the vehicle on charge, whereas a lead acid 288 $V$ – 40 $Ah$ battery pack, provided by Exide Technologies, is considered as representative of the ES buffer.

### *4.3 Main Power fluxes of the proposed architecture*

The demonstrator of charging station is designed to perform different operations, by means of the proper management of the power fluxes exchanged among the power converters and between the demonstrator and the main grid. A block scheme of the main power fluxes allowed with the realized architecture is reported in Figure 42 [38] [82] [67].

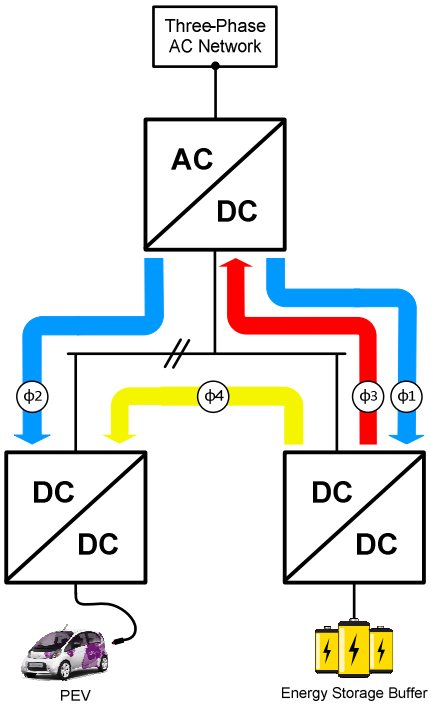


**Figure 42** *Main power fluxes of the laboratory prototype.*

As reported in the above figure, the AC/DC grid tied converter, by means of the power fluxes Φ1 and Φ2, can perform the low power charging operations both for the energy storage buffer and for PEV connected on charge, drawing energy from the main grid. In addition, thanks to its bidirectional topology, the grid-tied converter also allows V2G operations, taking advantage of the power flux Φ3.

On the DC side of the realized architecture the bidirectional DC/DC power converter can be properly controlled, in order to perform the following operations [67][7]:

- low power charging operations of the ES buffer, using the energy coming from the main grid, through the grid-tied converter, taking advantage of the power fluxΦ1;
- PEV charging operations in islanding configuration. In this case PEV battery pack can be charged by means of the power flux Φ4, without any power contribution from the main grid. In these operations no AC/DC conversion stage is performed;
- PEV charging operations supported by the power coming from both ES buffer and grid. In this case the PEV battery pack can be charged trough flux Φ3 and Φ4, with a strong reduction of the electric power requirement from the main grid;
- V2G operations supported by the power flux Φ3. These operative conditions are related to the connection of the bidirectional DC/DC converter with a four wheeled vehicle battery pack. The management of V2G operations involve the simultaneous control of both the AC/DC and DC/DC bidirectional converter.

Finally the charging operations of the considered PEV are managed through the proper control of the unidirectional DC/DC converter taking advantage of the power fluxes Φ2 and/or Φ4.

As described above, the proposed DC architecture is particularly suitable for the integration of RESs. In fact, the electric energy coming from DC voltage RESs, such as solar panels, can be directly supplied to the DC bus through high efficiency DC/DC converters. As shown in Figure 43, the energy coming from the renewable energy sources, through DC/DC power converters could flow towards the DC bus by means of the power flux Φ5. Then the same power flux can follow one or more power fluxes of Figure 42.

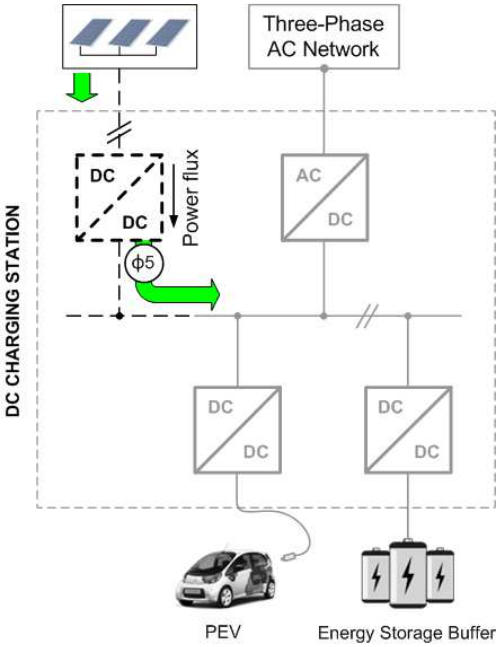


**Figure 43** *Main power fluxes for the proposed architecture with RESs.*

### *4.4 Control strategies of the prototype for fast charging and vehicle to grid operations*

Specific control strategies are implemented on the laboratory demonstrator in order to manage the power fluxes described in the above paragraph in different operative conditions. These control strategies can take advantage of the acquisition and control system whose main scheme is reported in Figure 44 [67].

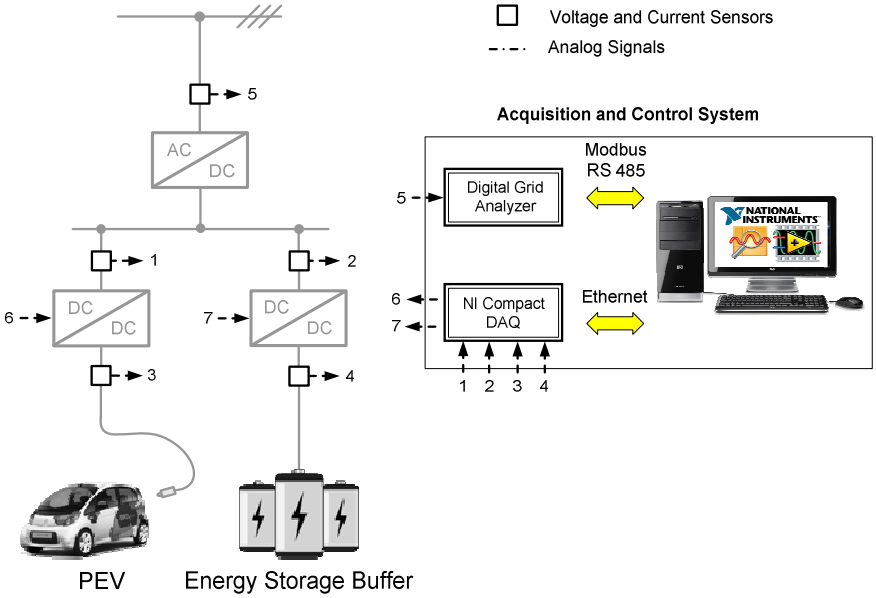


**Figure 44** *Block scheme of the laboratory acquisition and control system.*

In particular, the above scheme shows the measurement of the main electric parameters, which have been obtained through voltage and current sensors dislocated in different points of interest. The DC electric parameters are acquired through a National I/O Compact DAQ device, communicating with the supervising computer trough Ethernet protocol. The AC parameters are acquired by means of a Diris A40 digital grid analyzer, whose acquisition data can be read by the supervising computer trough ModBus RS485 communication protocol. The acquisition, filtering, monitoring and control of all electric parameters are realized by using a specific software interface realized in LabVIEW environment.

The control strategies of the power fluxes are implemented trough the simultaneous operations of both the on board embedded control of the power converters and external PI controllers, which are realized through the LabView interface on the supervising computer. In particular, in all the charging operations of PEV or buffer battery packs, involving the electric energy coming from the main grid, and in the V2G operations, the AC/DC bidirectional converter is controlled as a voltage source converter. In this case the control strategy can be performed by means of the embedded controller of the grid-tied converter, whose main operative scheme is reported in Figure 45 [67].

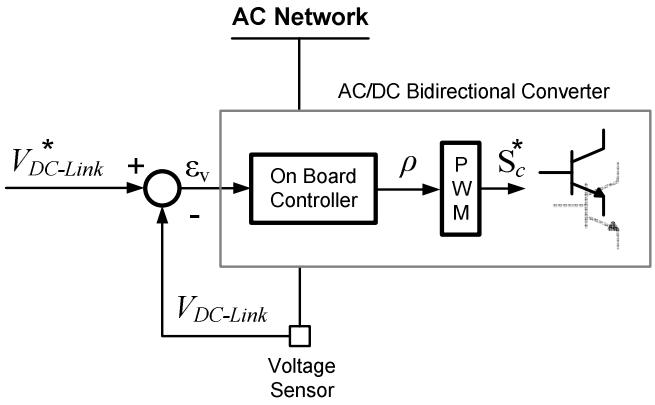


**Figure 45** *Control scheme of the bidirectional AC/DC power converter.*

As reported in the above scheme, the embedded controller, on the base of the error, $\varepsilon_v$, between the DC-Link voltage reference, $V^*_{DC\text{-}Link}$, and its measured value, $V_{DC\text{-}Link}$, generates a proper switching sequence, $S^*_c$, for the on board power devices, trough the PWM technique on the base of the evaluated modulation signal, $\rho$.

The control strategy realized for the unidirectional power converter, during the charging operations of PEVs is related to the management of the power fluxes Φ2 and Φ4 reported in Figure 42. The main control scheme of this converter is reported in Figure 46 [82] [67].

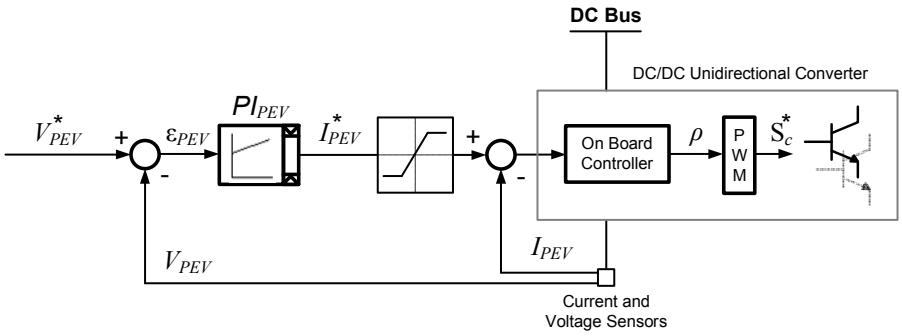


**Figure 46** *Control scheme of the unidirectional DC/DC power converter.*

In this case the vehicle charging current is controlled trough the embedded on board current controller, whereas its battery voltage is controlled trough an external control loop. In particular the external controller, $PI_{PEV}$, evaluates the error, $\varepsilon_{PEV}$, between the reference vehicle charging voltage, $V^*_{PEV}$, and its actual value, $V_{PEV}$, obtained through the voltage sensor on the vehicle side of the converter. On the

base of this comparison, the external controller evaluates the required PEV charging current, $I^*_{PEV}$, which is then limited trough a saturation block on the base of the maximum charging current desired. This current value is then used as reference value by the on board embedded controller of the unidirectional DC/DC power converter. Finally the embedded current controller evaluates the proper switching sequences for the on board power devices in order to track the reference current value $I^*_{PEV.}$

As already mentioned in this Chapter, the DC/DC bidirectional converter can be controlled both in DC-Link voltage reference and Energy Storage current reference mode. The first mode, which presents a control scheme similar to the case of the AC/DC converter described in Figure 45, is used to perform the islanding operative conditions. In this case the DC-Link is supplied by the only energy coming from the energy storage and its voltage reference value is set at 710 $V$. The energy storage current reference control mode is used in order to perform both vehicle to grid operative conditions and to support the main grid during the PEV fast charging operations which can be respectively controlled trough the power fluxes Φ3 and Φ4 reported in Figure 42. The main scheme of the control related to this last operative condition is reported in Figure 47 [67].

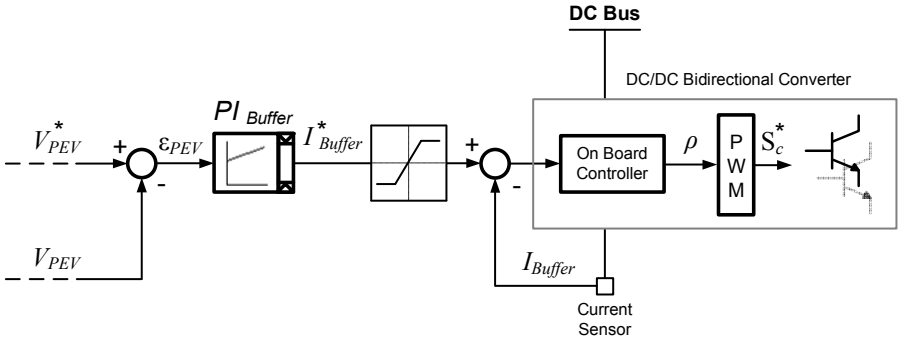


**Figure 47** *Control scheme of the bidirectional DC/DC converter during PEV fast charging operations.*

Also in this case the external control loop is based on the evaluation of the error, $\varepsilon_{PEV,}$ between the reference vehicle charging voltage, $V^*_{PEV}$, and its actual value, $V_{PEV}$. On the other hand the parameter of the controller, $PI_{Buffer}$, are tuned in order to obtain, as output, the reference discharging current of the energy storage buffer, $I^*_{Buffer}$. This reference value is then limited trough a saturation block, which takes into account the maximum discharging current allowed for the energy storage buffer. It is important to observe that, this reference value can be properly used for

the regulation of the electric power coming from the main grid during the vehicle charging operations. This is justified by the fact that the proposed grid-tied converter is controlled as a voltage source converter. Finally the embedded controller is devoted to the evaluation of the proper switching sequences of the on board power devices in order to track the current reference value $I^*_{Buffer.}$ In this way the evaluation of the energy storage buffer discharging current takes into account the electric power required both for the fast charging of the vehicle and for the reduction of the impact of this kind of operations on the main grid.

***Conclusions***

In this Chapter the design criteria and the realization of a laboratory prototype of fast DC charging architecture for PEVs have been analyzed. In particular, the main characteristics and topologies of DC/DC and AC/DC power converters have been identified, starting from preliminary evaluations based on a simplified Matlab-Simulink model. The description of the proposed architecture has shown the possibility of realizing different power fluxes mainly related to PEV fast charging, supported by stationary energy storage buffer, islanding and V2G operations. Finally the main control schemes of the power converters, supporting the above operative conditions, are reported with a detailed description of on board and external controllers.

# **Chapter 5.** Results and Discussion

### *Introduction*

This chapter is devoted to the discussion of the main results obtained during the research activities reported in this manuscript. In particular the first part is related to the characterization of different battery technologies, by means of the life cycle tester described in the Chapter 3. The discussion is focused in this case on the analysis of the main performance of the above battery modules during their discharging operations, for different constant current values. In addition experimental tests are carried out with the aim of evaluating the charging efficiency of each battery module for different charging rates. The second part of this chapter is aimed to analyse the performance figures of the realized prototype of DC fast charging station. In this case the experimental results are related to the main operative conditions obtained by means of the proper control of each converter, through the energy management strategies reported in Chapter 4.

### *5.1 Experimental Results on the performance of lithium batteries for PEVs*

The experimental results reported in this paragraph are related to the laboratory characterization of energy storage modules, obtained through the life cycle tester, described at the end of Chapter 3. In particular different charging and discharging tests have been performed on the $LiFePO_4$ and $Li[NiCoMn]O_2$ modules, whose main characteristics are reported in Table 3, in order to evaluate their main performance figures in comparison with a 12 *V*-40 *Ah* lead acid battery used as reference. The lead acid and the two lithium batteries, used to perform the tests described in this paragraph, have been preliminarily cycled up to a number of cycles corresponding at the 50% of their rated durability. The tests of this paragraph aim to analyze the behavior of the considered storage modules in terms of voltage drop, actual capacity, temperature and charging/discharging efficiency.

For the first set of tests each one of the three battery modules is separately charged with a constant current/constant voltage profile, setting a value of 4 *A* as current limit, which corresponds to a charging rate of 0.1 *C*. These charging procedures are repeated before each test and are stopped when the charging current is around zero for more than two hours. Starting from these preliminary conditions, after a resting period of about one hour, each battery module is completely discharged, with a constant current procedure, until it reaches the minimum discharging voltage suggested by the manufacturer. These discharging tests are performed at a constant current of 20 *A*, 40 *A*, and 60 *A*, following the same procedure. The results of these tests are respectively shown in Figure 48, Figure 49 and Figure 50 [57]. In these cases the battery voltage in *V* (Figures A) and the discharged capacity (Figures B), are evaluated as a ratio of their rated values reported in Table 3.

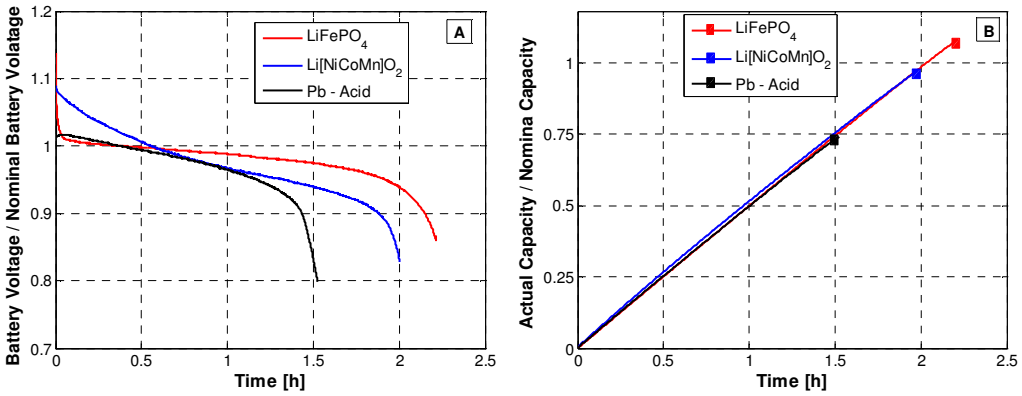

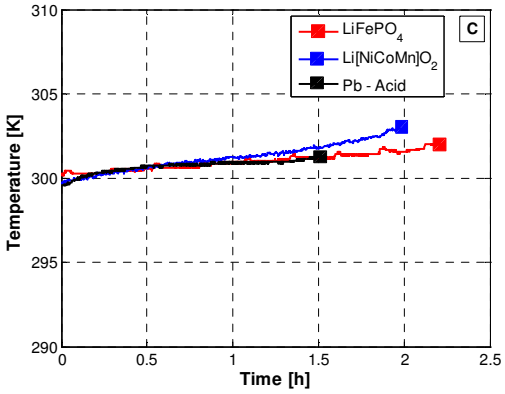


**Figure 48** *Discharging tests on $Li[NiCoMn]O_2$, $LiFePO_4$ and Pb batteries @ constant discharging current of 20 A.*

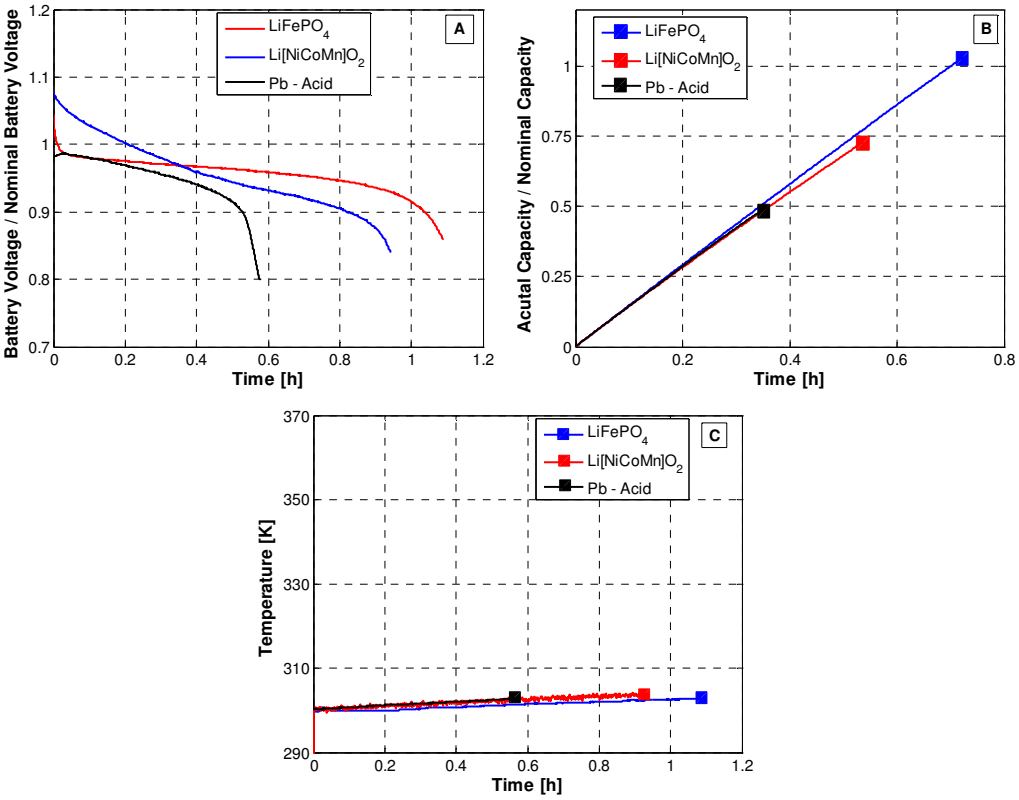


**Figure 49** *Discharging tests on $Li[NiCoMn]O_2$, $LiFePO_4$ and Pb batteries @ constant discharging current of 40 A.*

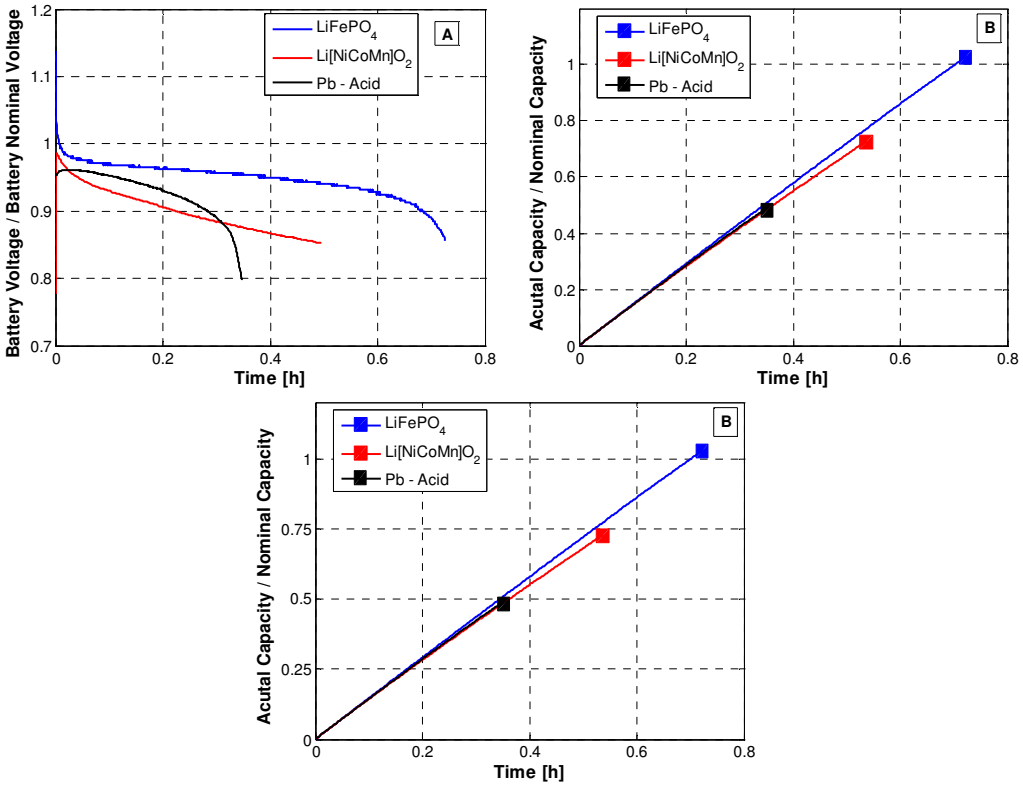


**Figure 50** *Discharging tests on Li[NiCoMn]$O_2$, $LiFePO_4$ and Pb batteries @ constant discharging current of 60 A.*

During these tests the voltage trends (Figures A) of the three modules analyzed present different behaviors. In particular $LiFePO_4$ chemistry shows an almost flat discharging voltage curve versus time, due to the cathodic process reversibility, associated with the similar structure of the two phases involved in Li insertion/extraction, i.e. $LiFePO_4$ and $FePO_4$ [66]. The reported behaviors of actual battery capacity (Figures B) are strongly affected by the discharging current values. In particular the highest reduction of actual capacity is evaluated for the lead acid batteries, especially at high discharging currents. In fact, the Pb storage module, in the discharging test @ 60 *A* reported in Figure 50, reduces the evaluated actual capacity up to 50% of its rated value. The same high discharging current test is less effective on both the lithium technologies, which present at the end of the test an actual capacity value quite similar to their rated capacity. In fact from Figure 50, it can be observed that an actual capacity value of about 75% for Li[NiCoMn]$O_2$ and around 100% for $LiFePO_4$ is reached. During the tests, the battery temperature is

measured on the external box of each battery module. The temperature increase observed during the discharge phase can be correlated to resistive dissipation of the conductive materials inside the storage modules, and to the exothermic nature of the discharge processes. The experimental results (Figures C) evidence that for the three types of batteries the temperature rising is in an acceptable range for the safety values suggested by the manufacturer [57].

Another set of tests is performed with the aim of evaluating the performance of the analyzed battery modules during the charging phases. For these tests the charging efficiency is evaluated, for different charging rates, as the actual value of the electric energy that is possible to obtain from each battery, during its discharging phase at a fixed current, with respect to the electric energy supplied during battery charging phase. These tests are carried out with charging rates ranging, from 0.05 *C* to 2 *C*, for the lithium batteries and from 0.05 *C* to 0.2 *C*, which corresponds to the maximum charging rate, for the lead acid battery. After each recharge the battery modules are discharged at a constant discharging rate of 0.2 *C*, in order to evaluate the charging efficiency, until the minimum discharging voltage is reached.

The results related to the above described tests are reported in Figure 51 A for the lithium batteries and in Figure 51 B for the lead acid battery. The reported results show the better performance of lithium technologies in terms of efficiency with respect to traditional Pb Technology. In particular, it can be observed that the efficiency values measured for the lithium batteries, at high charging rates, are quite similar to those evaluated for lead batteries at low charging rates [57].

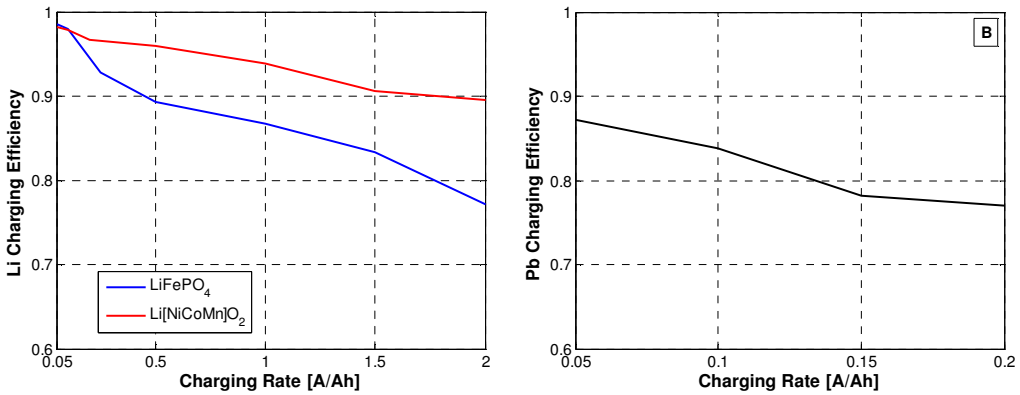


**Figure 51** *Charging efficiency of Li[NiCoMn]$O_2$, $LiFePO_4$, and Pb batteries versus charging rate.*

The results reported above evidence that $Li[NiCoMn]O_2$ storage modules are characterized by the highest charging efficiency in comparison with the other technologies analyzed in this manuscript. In fact they are characterized by efficiency values from 0.98, for low charging rates, to about 0.90, for higher charging rates. On the other the $LiFePO_4$ battery present charging efficiency values from 0.98 to 0.78 at the higher charging rate. This behaviour is clearly justified by the battery internal resistance, which is rather high for this kind of lithium module [68] [84]. However, in the real use of the $LiFePO_4$ batteries the strong degradation of performance, in terms of durability, for high values of charging rates, needs to be considered, as described in [26].

From the experimental results of the tests reported in this paragraph it follows that PEVs can take advantage of the behaviour of lithium compounds, in terms of high discharging and charging efficiency, in order to improve their travel range and charging times. For this reason experimental tests, on the same battery packs supplying electric power trains on standard driving cycle, have also been carried out. A description of these tests with the related results is reported in [57].

### *5.2 Experimental results on the laboratory prototype of DC fast charging architecture*

The experimental tests reported in this paragraph aim to characterize the laboratory prototype of DC fast charging architcture in its different operative conditions, taking advantage of the control schemes and energy management strategies described in the Chapter 4. All the tests reported in this paragraph are referred to the $LiFePO_4$ and Lead acid battery packs, whose main characteristics are reported in Table 6. In particular, before the beginning of each test, the $LiFePO_4$ battery pack, representing the vehicle on charge, has been preliminary discharged at a low constant current value of 4 A. On the other hand, the lead acid battery pack, representing the energy storage buffer, has been preliminarily charged with a $8\ A\ /330\ V$ constant current/constant voltage charging procedure. The discharging procedure for the $LiFePO_4$ battery pack is stopped when the minimum voltage value is reached, whereas the lead acid battery pack is considered fully charged when the charging current value is lower than $1\ A$ for more than one hour. The tests start after a resting period of about one hour for both the above battery packs. In addition, in order to avoid over-voltage conditions for the cells of the $LiFePO_4$ battery pack, its charging operations are stopped when the

SoC reaches the value of 95%[85]. The main results of the following tests have been reported also in [67].

The first test on the laboratory prototype is related to the charging operations of the $LiFePO_4$ battery pack using the electric power coming from the main grid. The charging test is performed, trough the flux Φ2 of Figure 42, by means of the proper control of AC/DC and unidirectional DC/DC converters, with a maximum current of 60 *A* corresponding to a charging rate of 1.5 *C*. The main results of this test are reported in Figure 52, which shows the typical CC/CV charging procedure obtained with the control scheme of Figure 46. In this case the maximum charging voltage of 61 *V* is reached at the end of the 60 *A* constant current phase (A). The active power supplied by the main grid during the charging procedure reaches the maximum value of 4.5 *kW*, corresponding to a vehicle charging power of 3.4 *kW* (B). In this case, the average conversion efficiency, $\eta_{avg}$, of the whole system can be evaluated as the ratio between electric energy supplied by the main grid and energy measured at the battery terminals. For this test a value of $\eta_{avg}$ = 0.76 and an average power factor of 0.94 have been evaluated [67].

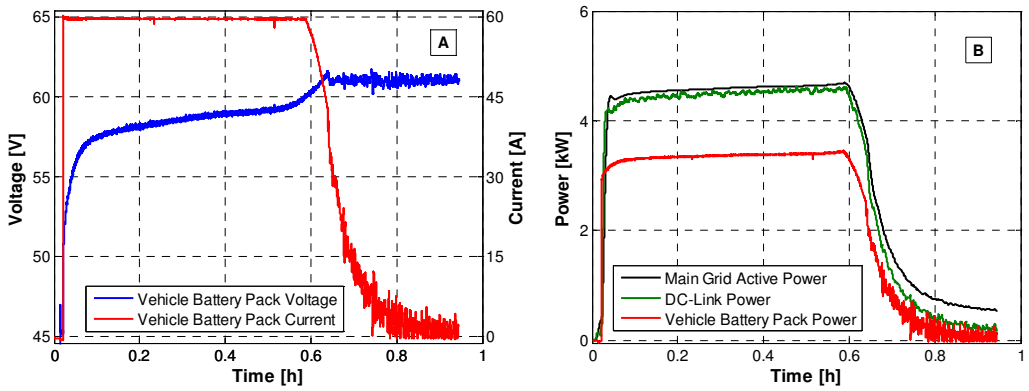


**Figure 52** *Voltage, Current and Power versus Time for the charging operation of 40 Ah $LiFePO_4$ battery pack at 60 A from the main grid.*

From the test reported above it can be deduced that the DC charging station prototype is able to perform fast charging times, reaching the value of SoC of about 80 % in about 35 *mins*. On the other hand the power requirements from the main grid needs to be properly taken into account for this charging operations. In fact typical commercial chargers for two-wheelers are characterized by a rated charging power of about 500 *W* [67], whereas in the above test the power supplied by the main grid is of about 4.5 *kW* (almost ten times higher). This aspect is particularly

relevant when vehicle of different sizes are simultaneously connected on charge. For the above reason a new set of tests, reported in the following, is performed with the aim to characterize the laboratory prototype in the charging operations supported by the electric power coming either from ES buffer, when the demonstrator works in islanding operative condition, or from ES buffer plus main grid.

The first test is related to the charging operations at 60 A of the $LiFePO_4$ battery pack with prototype working in islanding operative conditions. These operative conditions are performed, trough the power flux Φ4 of Figure 42 reported in Chapter 4, by means of the proper control of the two DC/DC converters. For this test the DC-Link is supplied by the electric power coming from the energy storage buffer. As a consequence the DC/DC bidirectional converter is controlled using the DC-Link voltage reference mode, with $V^*_{DC\text{-}Link}$ set at 710 *V*. On the other hand the DC/DC unidirectional converter is controlled as in the previous test, whereas the AC/DC grid tied converter is disabled. The main results of this test are reported in Figure 53.

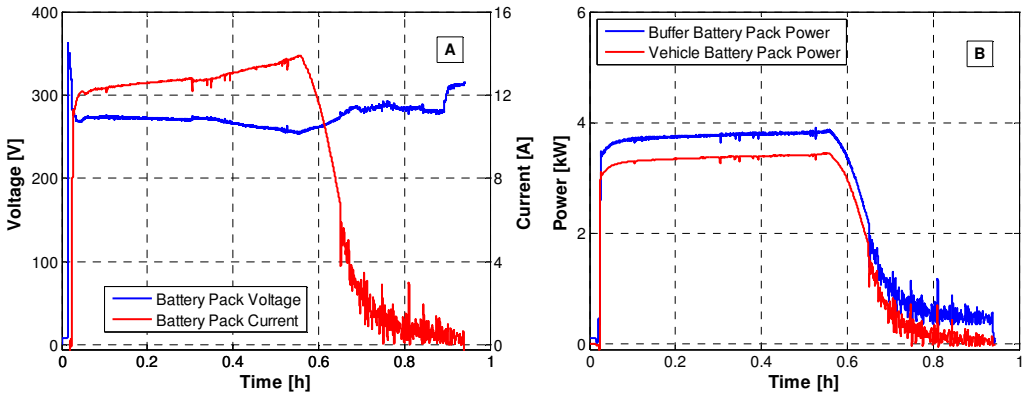


**Figure 53** *Voltage, Current and Power versus Time for the charging operation of 40 Ah $LiFePO_4$ battery pack at 60 A in islanding operative conditions.*

As shown by the reported results, after the first seconds of test, the buffer battery pack voltage drops down (A). This behaviour is justified by the sudden step of PEV battery pack current reference, $I^*_{PEV}$, imposed by the controller, $PI_{PEV}$, of the unidirectional DC/DC converter to start the vehicle charging operations. Then the voltage of the energy storage buffer decrease with a lower gradient until it reaches the value of 261 *V*, corresponding at the maximum discharging current of 14.7 *A*, at the end of the constant current charging phase of the vehicle battery pack. From a

comparison between the electric power coming from the energy storage buffer and the power incoming in the vehicle battery pack (B) it results that the same charging operation of the previous test is performed with a maximum power requirement from the energy storage buffer of about 3.85 *kW*. In this case an average conversion efficiency, $\eta_{avg}$ = 0.86, is evaluated as the ratio between the energy supplied to the EV battery pack and the energy coming from the storage buffer, both of them evaluated at the respective terminals [67].

The second experimental test of this set is related to the charging operation at 60 A of the $LiFePO_4$ battery pack, with the contribution of the main grid supported by the electric power coming from the energy storage buffer. This operative condition is performed taking advantage of the power fluxes Φ2 and Φ4 reported in Figure 42 of Chapter 4. The power withdrawn from the main grid can be limited trough the proper regulation of the ES buffer current reference, since the grid tied converter can be controlled only in voltage reference mode, following the scheme of Figure 45 with $V^*_{DC\text{-}Link}$ set in this case at 790 *V*. The ES buffer current is controlled by means of the DC/DC bidirectional converter, through its discharging current reference mode, with $I^*_{Buffer}$ set at a maximum value of 4 *A*. The main results of this test are reported in Figure 54 [67].

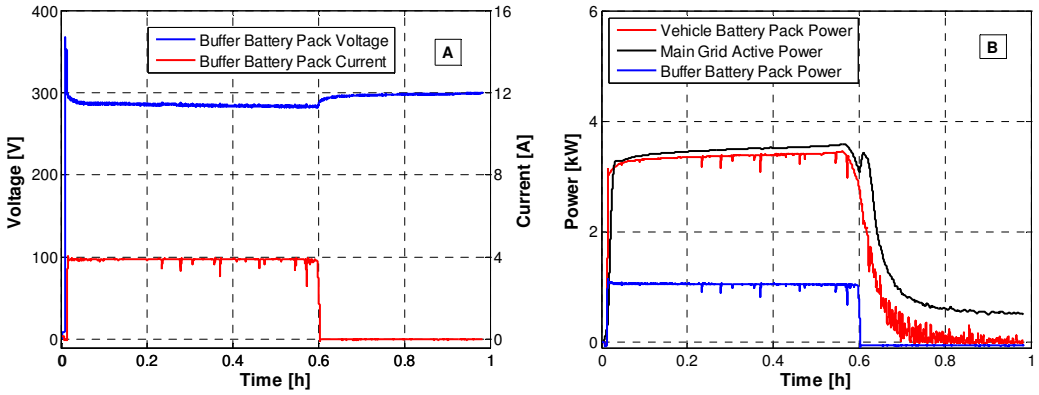


**Figure 54** *Voltage, Current and Power versus Time for the charging operation of 40 Ah $LiFePO_4$ battery pack at 60A supplied by main grid + energy storage buffer with $I^*_{Buffer}$ = 4A.*

In this test the buffer battery pack is discharged, during the first phase, at the maximum current value allowed of 4 *A*, reaching the minimum voltage value of 283 *V* (A) at the end of the constant current phase of the vehicle charging operation. The electric power coming from the main grid is limited, to the maximum value of 3.4 *kW*, by the electric power of 1 *kW* discharged by the ES

buffer (B). As a consequence the main grid active power is reduced of about 25% with respect to the test of Figure 52, where the vehicle is charged with the only energy coming from the main grid. The second part of the test is clearly related to the constant voltage phase, where the current values involved in the charging operations of the $LiFePO_4$ battery pack are limited by the reduced reference values imposed by the control system. For the main part of this test the grid tied converter works with a power factor of 0.9, whereas the whole system average conversion efficiency is $\eta_{avg} = 0.74$, evaluated as the ratio between the energy supplied to the $LiFePO_4$ battery pack and the energy coming from the main grid plus storage buffer [67].

The third test of this set is performed under the same operative conditions of the previous one but in this case a maximum discharging current reference of 12 *A* is set for the DC/DC bidirectional converter. The main results are reported in Figure 55.

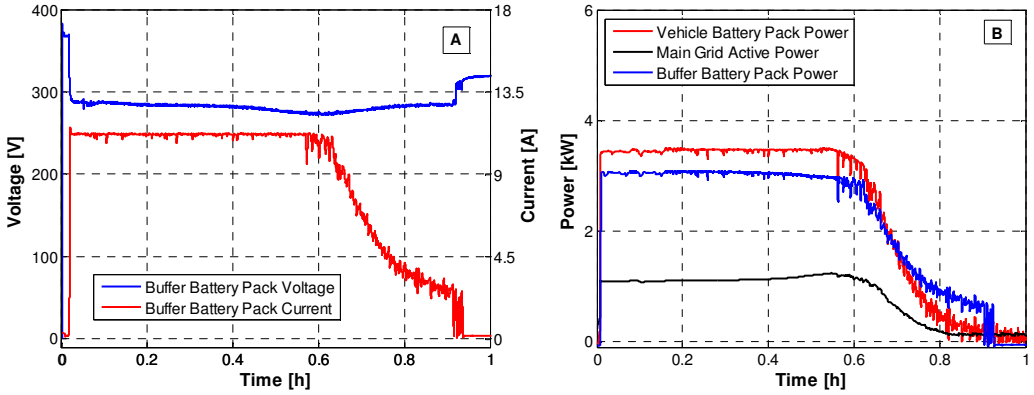


**Figure 55** *Voltage, Current and Power versus Time for the charging operation of 40 Ah $LiFePO_4$ battery pack at 60A supplied by main grid + energy storage buffer with $I^*_{Buffer} = 12A$.*

In this case the power requirement from the main grid are reduced up to 75% with respect to the case of Figure 52 thanks to the electric power supplied by the ES buffer, which reaches a maximum value of about 3 *kW* during the constant current phase of the $LiFePO_4$ charging operation (B). For this test, the grid-tied converter works at a power factor of about 0.58 and the whole system average efficiency, evaluated as the above test, is $\eta_{avg} = 0.82$.

A similar test has also been carried out in operative conditions, which are identical two the previous two tests, but with an ES buffer current reference value, $I^*_{Buffer}$, set at 8 *A*. The behaviour of electrical parameters is not reported in this

manuscript since it is quite similar to the previous two tests. In this case, the power factor for the grid tied converter is of about 0.8 and the average whole system conversion efficiency is $\eta_{avg} = 0.77$.

In order to summarize the tests reported in this paragraph on the laboratory prototype the main operative conditions and electrical parameters of each charging test are reported in Table 7.

| Charging Operation | Main Grid | ES Buffer +Main Grid | ES Buffer +Main Grid | ES Buffer +Main Grid | Islanding Mode |
|---|---|---|---|---|---|
| Vehicle Max. Charging Current [*A*] | 60 | 60 | 60 | 60 | 60 |
| Buffer Max. Discharging Current [*A*] | \ | 4 | 8 | 12 | 14 |
| Vehicle (Buffer) Battery Max Power [*kW*] | 3,4 (0) | 3,4 (1,14) | 3,4(2,22) | 3,4 (3,08) | 3,4 (3,85) |
| DC Bus Voltage [*V*] | 784 | 781 | 783 | 784 | 712 |
| DC Bus Max Power [*kW*] | 4,47 | 4,19 | 4,06 | 3,41 | 3,56 |
| Main Grid Max Active Power [*kW*] | 4,5 | 3,4 | 2,22 | 1,35 | \ |
| Avg Power Factor | 0,94 | 0,90 | 0,80 | 0,58 | \ |
| Avg Unidirectional DC/DC Efficiency [*p.u.*] | 0.77 | 0.83 | 0,90 | 0,92 | 0.94 |
| Avg Bidirectional DC/DC Efficiency [*p.u.*] | \ | 0.61 | 0.79 | 0.85 | 0.92 |
| Avg Bidirectional AC/DC Efficiency [*p.u.*] | 0,99 | 0.98 | 0,91 | 0.70 | \ |
| Whole system Avg Efficiency $\eta_{avg}$ [*p.u.*] | 0,76 | 0.74 | 0.77 | 0.82 | 0,86 |

**Table 7** *Main operative conditions and electrical parameters of the tests performed on the laboratory prototype.*

From the above table it is clear that, in the performed operative conditions, the laboratory prototype works with efficiency values, $\eta_{avg}$, which are always higher than 70 %. In particular, the highest values of efficiency are evaluated, for both the DC/DC unidirectional and bidirectional converters, in islanding operative conditions, when the charging operations are supported by the only electric power coming from the ES buffer and the DC-Link voltage reference, $V^*_{DC\text{-}Link}$, is set at 710 *V*. The slight decrease of efficiency related to the other operative conditions is justified by the fact that, when charging operations involve the main grid, the DC-Link voltage reference is set at 790 *V* by the control system of the grid-tied converter, increasing in this way the voltage conversion ratio between the DC-Link

and battery packs connected to the DC/DC converters. In addition, for these last operations, high current ripples, introduced by the grid-tied converter, can be considered cause of conduction losses (i.e., rms losses) [86][87]. For the same reasons the conversion efficiency of the two DC/DC converters decreases for higher electric power contributions from the main grid. As a consequence the highest value of $\eta_{avg}$, for the tests with ES buffer+main grid, is evaluated for the buffer discharging current of 12 A. Finally, the highest value of the power factor is measured when the vehicle charging operations are supplied only by the main grid, since the grid-tied converter works in this case closer to its rated operative conditions.

***Conclusions***

The results reported in this chapter are related to the experimental analysis of different battery modules during their charging/discharging operations and to the performance evaluation of the DC charging station laboratory prototype in its main operative conditions.

The experimental analysis of $Li[NiCoMn]O_2$ and $LiFePO_4$ battery modules have been carried out through the laboratory life cycle tester. In particular, the actual capacity for both the two lithium technologies have been evaluated as very close to their rated capacity also for high values of discharging current. On the other hand charging efficiency tests have shown better performance of $Li[NiCoMn]O_2$, in particular at high charging rate, with positive consequences on both regenerative breaking and fast charging operations.

From the experimental evaluations carried out on the laboratory prototype it follows that the use of stationary energy storage systems can perform a strong reduction of the impact of fast charging operations on the main grid. In addition, in all the operative conditions, an overall system efficiency higher than 70% has been evaluated, showing the real advantages of using DC architecture with only one AC/DC conversion stage. Finally experimental tests have shown that the higher is the contribution of the energy storage buffer the higher is the whole system efficiency.

## Conclusions and future work

In this manuscript reports the main design criteria, control strategies and experimental tests of DC fast charging architecture for full electric and plug-in hybrid vehicles are reported. The realized prototype presents different advantages, which are mainly related to the possibility of using high efficiency DC/DC power converters for an intelligent integration of PEVs, stationary energy storage buffer and renewable energy sources in a DC micro-grid configuration. With this kind of architecture the stationary energy storage buffers play an important role in supporting the main grid during PEV fast charging operations. Moreover V2G operations can be properly managed thanks to the bidirectional power fluxes of the considered power converters. Particular attention is also devoted to the description of the most recent energy storage technologies, such as battery and capacitors, which are considered particularly suitable to supply electric traction vehicles with good performance in terms of acceleration and autonomy. In this regard a laboratory test bench for experimental characterization of storage modules is introduced and described in order to analyze the behavior of the different storage units during fast charging and discharging operations.

Experimental results on the behaviour of the battery modules under test have shown the good performance of lithium technologies in terms of sicharging and charging efficiency. In fact the actual capacity for both the two lithium technologies have been evaluated as very close to their rated capacity also for high values of discharging current. On the other hand, both lithium technologies have shown a charging efficiency higher than 75% with charging rates up to 2 *C*.

In addition the different control strategies have been evaluated and tested on the laboratory prototype of DC charging architecture showing their effectiveness in the organization and management of the main power fluxes. The experimental results have evidenced in this case the advantages of using fast charging architecture based on DC bus with energy storage buffers. These advantages are mainly evidenced in terms of overall system efficiency and impact on the main grid, in the different operative conditions of the demonstrator. The convenience of using this kind of architecture become more relevant especially in case of simultaneous charging operations of a various number of vehicles of different size, which may not be supported by the main grid in its existing configurations.

Future activities are expected to be carried out both on the characterization of battery modules and on the experimental analysis of DC fast charging architecture. In particular the laboratory analysis of high energy density storage systems working in hybrid configuration with high power density devices, such as super-capacitors or LiC, is considered an attractive research activity since hybrid storage systems are expected to strongly improve the actual performance of PEVs. In addition future experimental activities on charging architecture based on the use of modular converters, integrated with single storage units, could further reduce the impact of fast charging operations on the main grid, in terms of power quality, and compensate the lack of experimental knowledge on the control of such complex distributed architecture.

## Acknowledgments

The author gratefully acknowledges Mr. Antonio Rossi, technician of Istituto Motori, for his assistance in running experimental tests and in drawing most of the figures of this manuscript.

# References


[1] J. Garcia-Villalobos, I. Zamora, J. S. Martin, F. Asensio and V. Aperribay, "Plug-in electric vehicles in electric distribution networks: A review of smart charging approaches," *Renewable and Sustainable Energy Reviews,* vol. 38, no. 0, pp. 717-731, 2014.

[2] A. E. Outlook and others, "Energy Information Administration," *Department of Energy,* 2010.

[3] G. Kalghatgi, "Developments in internal combustion engines and implications for combustion science and future transport fuels," *Proceedings of the Combustion Institute,* vol. 35, no. 1, pp. 101-115, 2015.

[4] J. W. Fergus, "Recent developments in cathode materials for lithium ion batteries," *Journal of Power Sources,* vol. 195, no. 4, pp. 939-954, 2010.

[5] A. \. K. Padhi, K. Nanjundaswamy and J. Goodenough, "Phospho-olivines as positive-electrode materials for rechargeable lithium batteries," *Journal of the electrochemical society,* vol. 144, no. 4, pp. 1188-1194, 1997.

[6] N. S. Pearre, W. Kempton, R. L. Guensler and V. V. Elango, "Electric vehicles: How much range is required for a day's driving?," *Transportation Research Part C: Emerging Technologies,* vol. 19, no. 6, pp. 1171-1184, 2011.

[7] S. Bai, D. Yu and S. Lukic, "Optimum design of an EV/PHEV charging station with DC bus and storage system," in *Energy Conversion Congress and Exposition (ECCE), 2010 IEEE*, 2010.

[8] H. Hoimoja, A. Rufer, G. Dziechciaruk and A. Vezzini, "An ultrafast ev charging station demonstrator," in *Power Electronics, Electrical Drives, Automation and Motion (SPEEDAM), 2012 International Symposium on*, 2012.

[9] Y. Dashora, J. W. Barnes, R. S. Pillai, T. Combs and M. Hilliard, "Optimized energy management for large organizations utilizing an on-site PHEV fleet, storage devices and renewable electricity generation," *Energy Systems,* vol. 3, no. 2, pp. 133-151, 2012.

[10] J. Lopes, F. Soares and P. Almeida, "Integration of Electric Vehicles in the Electric Power System," *Proceedings of the IEEE,* vol. 99, no. 1, pp. 168-183, 2011.

[11] B. M. Al-Alawi and T. H. Bradley, "Review of hybrid, plug-in hybrid, and electric vehicle market modeling Studies," *Renewable and Sustainable Energy Reviews ,* vol. 21, no. 0, pp. 190-203, 2013.

[12] "UNRAE," [Online]. Available: www.unrae.it.

[13] J. Massiani, "Cost-Benefit Analysis of policies for the development of electric vehicles in Germany: Methods and results," *Transport Policy,* vol. 38, no. 0, pp. 19-26, 2015.

[14] G. Chun-lin, L. Wu, W. Dan and Q. Wen-bo, "Impact of electric vehicle charging on power grid," in *International Conference on Electrical and Control Engineering (ICECE)*, 2011.

[15] N. Keisuke, S. Tohno, M. Kono and M. Kasahara, "Effects of electric vehicles (EV) on environmental loads with consideration of regional differences of electric power generation

and charging characteristic of EV users in Japan," *Applied Energy,* vol. 71, no. 2, pp. 111-125, 2002.

[16] O. Erdinc, O. Elma, M. Uzunoglu, U. Selamogullari, B. Vural, E. Ugur, A. Boynuegri and S. Dusmez, "Experimental performance assessment of an online energy management strategy for varying renewable power production suppression," *International Journal of Hydrogen Energy,* vol. 37, no. 6, pp. 4737-4748, 2012.

[17] N. A. Ahmed, M. Miyatake and A. Al-Othman, "Power fluctuations suppression of stand-alone hybrid generation combining solar photovoltaic/wind turbine and fuel cell systems," *Energy Conversion and Management,* vol. 49, no. 10, pp. 2711-2719, 2008.

[18] F. Mwasilu, J. J. Justo, E.-K. Kim, T. D. Do and J.-W. Jung, "Electric vehicles and smart grid interaction: A review on vehicle to grid and renewable energy sources integration," *Renewable and Sustainable Energy Reviews,* vol. 34, no. 0, pp. 501-516, 2014.

[19] M. A. Eltawil and Z. Zhao, "Grid-connected photovoltaic power systems: Technical and potential problems - A review," *Renewable and Sustainable Energy Reviews,* vol. 14, no. 1, pp. 112-129, 2010.

[20] V. Calderaro, G. Conio, V. Galdi, G. Massa and A. Piccolo, "Active management of renewable energy sources for maximizing power production," *International Journal of Electrical Power & Energy Systems,* vol. 57, no. 0, pp. 64-72, 2014.

[21] V. Gungor, D. Sahin, T. Kocak, S. Ergut, C. Buccella and C. &. H. G. Cecati, "A Survey on Smart Grid Potential Applications and Communication Requirements," *Industrial Informatics, IEEE Transactions on,* vol. 9, pp. 28-42, 2013.

[22] B. Battke, T. S. Schmidt, D. Grosspietsch and V. H. Hoffmann, "A review and probabilistic model of lifecycle costs of stationary batteries in multiple applications," *Renewable and Sustainable Energy Reviews ,* vol. 25, no. 0, pp. 240-250, 2013.

[23] D. B. Richardson, "Electric vehicles and the electric grid: A review of modeling approaches, Impacts, and renewable energy integration," *Renewable and Sustainable Energy Reviews ,* vol. 19, no. 0, pp. 247-254, 2013.

[24] E. Sortomme and M. A. El-Sharkawi, "Optimal scheduling of vehicle-to-grid energy and ancillary services," *Smart Grid, IEEE Transactions on,* vol. 3, no. 1, pp. 351-359, 2012.

[25] E. Sortomme and M. A. El-Sharkawi, "Optimal Charging Strategies for Unidirectional Vehicle-to-Grid.," *IEEE Trans. Smart Grid,* vol. 2, no. 1, pp. 131-138, 2011.

[26] N. Omar, M. A. Monem, Y. Firouz, J. Salminen, J. Smekens, O. Hegazy, H. Gaulous, G. Mulder, P. V. den Bossche, T. Coosemans and J. V. Mierlo, "Lithium iron phosphate based battery - " Assessment of the aging parameters and development of cycle life model," *Applied Energy,* vol. 113, no. 0, pp. 1575-1585, 2014.

[27] C. Quinn, D. Zimmerle and T. H. Bradley, "The effect of communication architecture on the availability, reliability, and economics of plug-in hybrid electric vehicle-to-grid ancillary services," *Journal of Power Sources ,* vol. 195, no. 5, pp. 1500-1509, 2010.

[28] S. Habib, M. Kamran and U. Rashid, "Impact analysis of vehicle-to-grid technology and

charging strategies of electric vehicles on distribution networks - A review," *Journal of Power Sources,* vol. 277, no. 0, pp. 205-214, 2015.

[29] M. D. Galus, M. G. Vaya, T. Krause and G. Andersson, "The role of electric vehicles in smart grids," *Wiley Interdisciplinary Reviews: Energy and Environment,* vol. 2, no. 4, pp. 384-400, 2013.

[30] S. D. McArthur, E. M. Davidson, V. M. Catterson, A. L. Dimeas, N. D. Hatziargyriou, F. Ponci and T. Funabashi, "Multi-agent systems for power engineering applications—Part I: Concepts, approaches, and technical challenges," *Power Systems, IEEE Transactions on,* vol. 22, no. 4, pp. 1743-1752, 2007.

[31] M. Wooldridge and N. R. Jennings, "Intelligent agents: Theory and practice," *The knowledge engineering review,* vol. 10, no. 02, pp. 115-152, 1995.

[32] "Colonnine elettriche: Colonnine di ricarica per veicoli elettrici," 2014. [Online]. Available: http://www.colonnineelettriche.it. [Accessed 09 03 2015].

[33] McKinsey & Company, "Electric vehicles in Europe:gearing up for a new phase?," 2013.

[34] "SAE Electric Vehicle and Plug in Hybrid Electric Vehicle Conductive Charge Coupler J1772," 2012.

[35] M. Yilmaz and P. T. Krein, "Review of charging power levels and infrastructure for plug-in electric and hybrid vehicles," in *Electric Vehicle Conference (IEVC), 2012 IEEE International*, 2012.

[36] "CHAdeMO Association," 2015. [Online]. Available: http://www.chademo.com/.

[37] S. Bakker, P. Leguijt and H. van Lente, "Niche accumulation and standardization - the case of electric vehicle recharging plugs," *Journal of Cleaner Production,* no. 0, pp. -, 2015.

[38] O. Veneri, L. Ferraro, C. Capasso and D. Iannuzzi, "Charging infrastructures for EV: Overview of technologies and issues," in *Electrical Systems for Aircraft, Railway and Ship Propulsion (ESARS), 2012*, 2012.

[39] N. Savage and R. R. Nordhaus, "Jamieson “DC micro grids: Benefits and Barriers”," *Analyses written at the request of REIL.*

[40] M. A. Perez, S. Bernet, J. Rodriguez, S. Kouro and R. Lizana, "Circuit topologies, modelling, control schemes and applications of modular multilevel converters," 2014.

[41] A. K. Sahoo, R. Otero-De-Leon and N. Mohan, "Review of modular multilevel converters for teaching a graduate-level course of power electronics in power systems," in *North American Power Symposium (NAPS), 2013*, 2013.

[42] V. F. Pires, E. Romero-Cadaval, D. Vinnikov, I. Roasto and J. Martins, "Power converter interfaces for electrochemical energy storage systems--A review," *Energy Conversion and Management,* vol. 86, pp. 453-475, 2014.

[43] F. Peng and J. Lai, *Multilevel cascade voltage source inverter with seperate DC sources,* Google Patents, 1997.

[44] L. Maharjan, S. Inoue, H. Akagi and J. Asakura, "State-of-charge (SOC)-balancing control of a

battery energy storage system based on a cascade PWM converter," *Power Electronics, IEEE Transactions on,* vol. 24, no. 6, pp. 1628-1636, 2009.

[45] I. Trintis, S. Munk-Nielsen and R. Teodorescu, "A new modular multilevel converter with integrated energy storage," in *IECON 2011-37th Annual Conference on IEEE Industrial Electronics Society*, 2011.

[46] L. Maharjan, S. Inoue, H. Akagi and J. Asakura, "A transformerless battery energy storage system based on a multilevel cascade PWM converter," in *Power Electronics Specialists Conference, 2008. PESC 2008. IEEE*, 2008.

[47] F. Ciccarelli, A. Del Pizzo and D. Iannuzzi, "An ultra-fast charging architecture based on modular multilevel converters integrated with energy storage buffers," in *Ecological Vehicles and Renewable Energies (EVER), 2013 8th International Conference and Exhibition on*, 2013.

[48] M. Vasiladiotis, A. Rufer and A. Beguin, "Modular converter architecture for medium voltage ultra fast EV charging stations: Global system considerations," in *Electric Vehicle Conference (IEVC), 2012 IEEE International*, 2012.

[49] Z. Rezvani, J. Jansson and J. Bodin, "Advances in consumer electric vehicle adoption research: A review and research agenda," *Transportation research part D: transport and environment,* vol. 34, pp. 122-136, 2015.

[50] M. Gaberscek, *Lithium Batteries. Advanced Technologies and Applications. Edited by Bruno Scrosati, KM Abraham, Walter van Schalkwijk and Jusef Hassoun.,* Wiley Online Library, 2014.

[51] A. Nguyen, J. Lauber and M. Dambrine, "Optimal control based algorithms for energy management of automotive power systems with battery/supercapacitor storage devices," *Energy Conversion and Management,* vol. 87, pp. 410-420, 2014.

[52] R. Araujo, R. de Castro, C. Pinto, P. Melo and D. Freitas, "Combined Sizing and Energy Management in EVs With Batteries and Supercapacitors," 2014.

[53] T. R. Jow, K. Xu, O. Borodin and M. Ue, Electrolytes for lithium and lithium-ion batteries, vol. 58, Springer, 2014.

[54] S. Sivakkumar and A. Pandolfo, "Carbon nanotubes/amorphous carbon composites as high-power negative electrodes in lithium ion capacitors," *Journal of Applied Electrochemistry,* vol. 44, no. 1, pp. 105-113, 2014.

[55] N. Sharma and M. Wagemaker, "Lithium-Ion Batteries," in *Neutron Applications in Materials for Energy*, Springer, 2015, pp. 139-203.

[56] P. Corbo, F. Migliardini and O. Veneri, Hydrogen fuel cells for road vehicles, Springer Science \& Business Media, 2011.

[57] C. Capasso and O. Veneri, "Experimental analysis on the performance of lithium based batteries for road full electric and hybrid vehicles," *Applied Energy,* vol. 136, pp. 921-930, 2014.

[58] S. Piller, M. Perrin and Jossen, "Methods for state-of-charge determination and their applications," *Journal of power sources,* vol. 96, no. 1, pp. 113-120, 2001.

[59] S. Rodrigues, N. Munichandraiah and A. Shukla, "A review of state-of-charge indication of batteries by means of ac impedance measurements," *Journal of power Sources,* vol. 87, no. 1, pp. 12-20, 2000.

[60] M. A. Delucchi and T. E. Lipman, "An analysis of the retail and lifecycle cost of battery-powered electric vehicles," *Transportation Research Part D: Transport and Environment,* vol. 6, no. 6, pp. 371-404, 2001.

[61] B. Zakeri and S. Syri, "Electrical energy storage systems: A comparative life cycle cost analysis," *Renewable and Sustainable Energy Reviews,* vol. 42, pp. 569-596, 2015.

[62] S. Dhameja, Electric vehicle battery systems, Newnes, 2001.

[63] K. R. Bullock, "Lead/acid batteries," *Journal of power sources,* vol. 51, no. 1, pp. 1-17, 1994.

[64] O. Veneri, F. Migliardini, C. Capasso and P. Corbo, "Dynamic behaviour of Li batteries in hydrogen fuel cell power trains," *Journal of Power Sources,* vol. 196, no. 21, pp. 9081-9086, 2011.

[65] A. Vezzini, "Lithium-Ion Battery Management," *Lithium-Ion Batteries: Advances and Applications,* p. 345, 2013.

[66] S. Adams, "Ultrafast lithium migration in surface modified LiFePO 4 by heterogeneous doping," *Applied Energy,* vol. 90, no. 1, pp. 323-328, 2012.

[67] O. Veneri, C. Capasso and D. Iannuzzi, "Experimental Study of a DC Charging Station for Fully-Electrified Low-Power Two-Wheeler," *Applied Energy (Accepted for Pubblication),* 2015.

[68] B. Scrosati and J. Garche, "Lithium batteries: Status, prospects and future," *Journal of Power Sources,* vol. 195, no. 9, pp. 2419-2430, 2010.

[69] A. Prakash, P. Manikandan, K. Ramesha, M. Sathiya, J. Tarascon and A. Shukla, "Solution-combustion synthesized nanocrystalline Li4Ti5O12 as high-rate performance Li-ion battery anode," *Chemistry of Materials,* vol. 22, no. 9, pp. 2857-2863, 2010.

[70] A. Sivashanmugam, S. Gopukumar, R. Thirunakaran, C. Nithya and S. Prema, "Novel Li 4 Ti 5 O 12/Sn nano-composites as anode material for lithium ion batteries," *Materials Research Bulletin,* vol. 46, no. 4, pp. 492-500, 2011.

[71] G.-N. Zhu, Y.-G. Wang and Y.-Y. Xia, "Ti-based compounds as anode materials for Li-ion batteries," *Energy \& Environmental Science,* vol. 5, no. 5, pp. 6652-6667, 2012.

[72] M. Winter and R. J. Brodd, "What are batteries, fuel cells, and supercapacitors?," *Chemical reviews,* vol. 104, no. 10, pp. 4245-4270, 2004.

[73] R. Kotz and M. Carlen, "Principles and applications of electrochemical capacitors," *Electrochimica Acta,* vol. 45, no. 15, pp. 2483-2498, 2000.

[74] P. Sharma and T. Bhatti, "A review on electrochemical double-layer capacitors," *Energy Conversion and Management,* vol. 51, no. 12, pp. 2901-2912, 2010.

[75] L. L. Zhang and X. Zhao, "Carbon-based materials as supercapacitor electrodes," *Chemical Society Reviews,* vol. 38, no. 9, pp. 2520-2531, 2009.

[76] Y. Wang, Z. Shi, Y. Huang, Y. Ma, C. Wang, M. Chen and Y. Chen, "Supercapacitor devices based on graphene materials," *The Journal of Physical Chemistry C,* vol. 113, no. 30, pp. 13103-13107, 2009.

[77] Y. Firouz, N. Omar, J. M. Timmermans, P. Van den Bossche and J. Van Mierlo, "Lithium-ion capacitor - Characterization and development of new electrical model," *Energy,* p. In press, 2015.

[78] P. H. Smith, T. N. Tran, T. L. Jiang and J. Chung, "Lithium-ion capacitors: Electrochemical performance and thermal behavior," *Journal of Power Sources,* vol. 243, pp. 982-992, 2013.

[79] O. Veneri, F. Migliardini, C. Capasso and P. Corbo, "Experimental performance assessment of Pb, Li [NiCoMn] O 2 and LiFePO 4 batteries for road vehicles," in *Power Electronics, Electrical Drives, Automation and Motion (SPEEDAM), 2012 International Symposium on*, 2012.

[80] S. Li, K. Bao, X. Fu and H. Zheng, "Energy management and control of electric vehicle charging stations," *Electric Power Components and Systems,* vol. 42, no. 3-4, pp. 339-347, 2014.

[81] Y. Sun, W. Liu, M. Su, X. Li, H. Wang and J. Yang, "A unified modeling and control of a multi-functional current source-typed converter for V2G application," *Electric Power Systems Research,* vol. 106, pp. 12-20, 2014.

[82] O. Veneri, C. Capasso, L. Ferraro and A. Del Pizzo, "Performance analysis on a power architecture for EV ultra-fast charging stations," in *Clean Electrical Power (ICCEP), 2013 International Conference on*, 2013.

[83] S. Oliveira and I. Barbi, "A three-phase step-up DC-DC converter with a three-phase high frequency transformer," in *Industrial Electronics, 2005. ISIE 2005. Proceedings of the IEEE International Symposium on*, 2005.

[84] P. Axmann, C. Stinner, M. Wohlfahrt-Mehrens, A. Mauger, F. Gendron and C. Julien, "Nonstoichiometric LiFePO4: defects and related properties," *Chemistry of Materials,* vol. 21, no. 8, pp. 1636-1644, 2009.

[85] R. C. Cope and Y. Podrazhansky, "The art of battery charging," in *Battery Conference on Applications and Advances, 1999. The Fourteenth Annual*, 1999.

[86] S. Zhou and G. A. Rincon-Mora, "A high efficiency, soft switching DC-DC converter with adaptive current-ripple control for portable applications," *Circuits and Systems II: Express Briefs, IEEE Transactions on,* vol. 53, no. 4, pp. 319-323, 2006.

[87] R. Jaschke, "Conduction Losses in DC/DC-Converters as buckboost/boostbuck synchronous rectifier types," in *Compatibility in Power Electronics, 2007. CPE'07*, 2007.